Summer 8-2022

Upland Migration of Coastal Marshes as a Response to Sea Level Rise and Fire Management: Past, Present, and Predicted

Devin Jen

UPLAND MIGRATION OF COASTAL MARSHES AS A RESPONSE TO SEA LEVEL RISE AND FIRE MANAGEMENT: PAST, PRESENT, AND PREDICTED

by

Devin Renee Jen

A Thesis
Submitted to the Graduate School,
the College of Arts and Sciences
and the School of Ocean Science and Engineering
at The University of Southern Mississippi
in Partial Fulfillment of the Requirements
for the Degree of Master of Science

Approved by:

Dr. Wei Wu, Committee Chair
Dr. Patrick Biber
Dr. Kevin Dillon

August 2022

ABSTRACT

Coastal marshes are one of the most productive and intensively used ecosystems in the world, providing numerous ecosystem services that are critical to the communities that surround them and beyond. However, they are under threat due to a variety of natural and anthropogenic stressors, such as sea level rise (SLR). SLR can cause marshes to drown, converting them to open water. Marshes can respond to SLR through landward migration when suitable geomorphological condition and habitat are available. My research focuses on the landward migration pattern and mechanisms including the role of proscribed fire. I evaluated the historical land cover changes at the Grand Bay National Estuarine Research Reserve and the Pascagoula River delta over two-time intervals since 1955 and specifically focused on the forest-marsh dynamics. I found that while there were areas of forest transitioning to marsh and the rates of these transitions increased from the first-time interval to the second, gains in marsh area cannot keep up with the amount of marsh lost to forest or water. I then used a mechanistic model to predict soil porewater salinity under different SLR scenarios and found that the maximum salinity band will move up the elevation gradient as sea level increases. This supports landward migration as salinity stress will continue to move up in elevation potentially freeing spaces for marshes to migrate into. Using Bayesian multi-level models, I found that fire management likely helps facilitate landward migration of coastal marshes by increasing productivity of salt marsh and understory vegetation in ecotone and upland forests as well as decreasing tree height growth through increased salinity stress. My findings provide insights as to how marshes respond to SLR and fire management.

ACKNOWLEDGMENTS

I would like to thank my advisor Dr. Wei Wu for her patience, support, and guidance throughout this project as well as my committee members Dr. Patrick Biber and Dr. Kevin Dillon for their advice and feedback. This work could not have been completed without the funding provided by the Mississippi-Alabama Sea Grant and the help and support of my lab members: Dr. Hailong Huang, Makenzie Holifield, Evan Grimes, Kodi Feldpausch, Kelly San Antionio, Megan Ringate, and Ethan Ramsey. I would also like to thank those that provided the maps for the land cover change analysis. This included Dr. Loretta Battaglia at Texas A&M University - Corpus Christi who provided 1955 and 1988 NWI maps of the Grand Bay National Estuarine Research Reserve (GBNERR), Dr. Jonathan Pitchford who provided 2015 land cover map and other GIS data for the GBNERR, and Dr. Carter and Margaret Waldron who provided land cover maps for the Pascagoula River delta.

DEDICATION

This thesis is dedicated to my parents for providing endless support and encouragement, not just through this entire process, but for everything I have ever tried to accomplish and my partner, Evan Engels, for standing by me over the last two years.

TABLE OF CONTENTS

LIST OF TABLES

LIST OF ILLUSTRATIONS

CHAPTER I – HISTORICAL LAND COVER CHANGES AT RIVERINE VS. MARINE DOMINATED ESTUARIES IN SOUTHEASTERN MISSISSIPPI – FOREST-MARSH DYNAMICS

1.1 Introduction

Coastal marshes are one of the most productive and intensively used ecosystems in the world, providing numerous ecosystem services that are critical to the communities that surround them as well as globally beneficial (Costanza et al., 1997; Battaglia et al., 2012). Coastal marshes sequester a significant amount of carbon with current estimates of carbon storage by coastal mashes in the contiguous United States around 0.44 Tg C per year (Morris et al., 2012). Many species of wildlife are dependent on the coastal marshes of the Northern Gulf of Mexico (NGOM), with 13 species or subspecies endemic to this region (Battaglia et al., 2012). Numerous birds utilize the NGOM with 40 species of waterfowl and 90% of all bird species in eastern North America having been observed here (Lowery and Newman, 1954; Battaglia et al., 2012). Furthermore, these marshes provide important nursery habitat for many economically important fisheries. Between 2000 and 2004 over 8 billion pounds of fish and shellfish were landed in the Gulf of Mexico, of that, 97% by weight were from estuarine dependent fish and shellfish such as blue crab, red drum, brown shrimp, and spotted sea trout (Lellis-Dibble et al., 2008; Environmental Protection Agency, 2015). Coastal marsh vegetation plays an important role in protection from hazards such as storms through wave attenuation and erosion through shoreline stabilization and vertical accretion (Shepard et al., 2011; Barbier et al., 2013). Finally, coastal wetlands provide many recreational opportunities. In the five

NGOM states, 22.4 billion was spent on wildlife related recreation from 1999-2003 (Battaglia et al., 2012).

Coastal marshes have experienced extensive loss globally due to climate change as well as other natural and anthropogenic stressors with 50% of coastal marshes worldwide facing loss or degradation (Barbier et al., 2011). In the contiguous United States, over half of the coastal wetlands are found around the NGOM region and account for ~71% of the coastal wetland loss between 2004 and 2009 (Field, 1991; Engle, 2011; Dahl and Stedman, 2013). As coastal marshes are positioned within narrow elevation ranges in the intertidal zone, sea level rise (SLR) in particular poses a threat to them (Mogenson and Rogers, 2018; Wu et al., 2020). SLR has accelerated in recent decades from 1.4 mm/year in the early 20th century, to 3.6 mm/year between 2006-2015 (Lindsey, 2020; Burns et al., 2021). The increased inundation from SLR can cause marshes to drown, converting them to open water (Shirley and Battaglia, 2006). Between 1998 and 2009, the majority of the coastal wetland area lost was due to inundation and saltwater intrusion, causing wetlands to convert to open water (Stedman and Dahl, 2008; Dahl and Stedman, 2013).

Relative sea level rise (RSLR), which includes subsidence, can exacerbate this problem by creating much higher local rates of sea level rise (Shirley and Battaglia, 2006; Penland and Ramsey, 1990). For example, Louisiana which has the highest rate of RSLR in the NGOM at 10.4 mm/year accounts for 40% of the wetlands in the contiguous US and ~80% of the total wetland loss (Penland and Ramsey, 1990; Bourne, 2000). Mississippi which has a RSLR rate of 4.68 mm/year has also seen losses of coastal marshes to open water in the Pascagoula River delta (Pascagoula) and the Grand Bay

National Estuarine Research Reserve (GBNERR) since 1955 (NOAA Tides and Currents; Orson et al., 1985; Shirley and Battaglia, 2006; Nicholson, 2017; Waldron et al., 2021).

There are ways in which marshes can maintain themselves despite rising sea levels. This is achieved by building the marsh platform in the vertical direction through vertical accretion and/or in the horizontal direction through landward migration (Kirwan et al., 2016). The rate of vertical accretion is based on the vegetations' ability to trap and accumulate sediments through above- and belowground biomass which, in turn, can raise the elevation of the platform (Shirley and Battaglia, 2006; Kirwan et al., 2010; Wu et al., 2020). Aboveground biomass can attenuate wave action and trap sediments that are suspended in the water column. Additionally, dead organic matter from aboveground biomass can accumulate and contribute to building the marsh platform. Similarly, the growth and die-off of the vegetations' root systems can add organic matter and raise the marsh platform (Kirwan and Megonigal, 2013). The rate of vertical accretion being equal or exceeding that of RSLR is necessary for marshes to maintain their position. Because of this, sediment inputs are critical for building the marsh platform. A study by Jankowski et al. (2017) found 65% of wetlands in the Mississippi Delta can maintain themselves through vertical accretion at a RSLR rate of 12 mm/year. Wu et al. (2020) found that the GBNERR and Pascagoula had SLR thresholds of 7.2 mm/year and 10.3 mm/year, respectively. This difference of 3.1 mm/year was largely attributed to greater fluvial sediment input at Pascagoula.

In the horizontal direction, marshes can migrate landward or transgress. Due to SLR, higher saline water will reach upland areas that previously did not receive tidal inundation. These high marsh and upland areas are characterized by glycophytes. The

increase in soil porewater salinity from the incoming tide can increase salinity stress and cause the vegetation at these higher elevations to die off - creating space that the more halophytic marsh vegetation can then migrate into (Brinson et al., 1995; Donnelly and Bertness, 2001; Kirwan et al., 2016). However, some studies have found that the forest area may be more resistant to inundation or that mature trees will be unaffected, but the recruitment of new individuals will be impacted (Kirwan et al., 2007; Field et al., 2016). Should this be the case, landward migration would be stepwise or an ecological ratchet (Kearney et al. 2019). Other impediments to marsh migration would be anthropogenic barriers or a steep elevational slope (Battaglia et al., 2012; Field et al., 2016; Kirwan et al., 2016; Borchert et al. 2018). It is important to understand historical trends of land cover change in order to predict how coastal marshes will respond to SLR for a given area. In this chapter, I will assess the historical land cover change since 1955 at the GBNERR and Pascagoula estuaries which represent areas that have very limited (GBNERR) and rich (Pascagoula) fluvial inputs. Overarchingly, this chapter seeks to evaluate and compare the historical land cover change over two-time intervals: 1955-1988 and 1988-2015 for GBNERR and 1955-1996 and 1996-2014 for Pascagoula. More specifically, with this study I aim to identify the land cover types that have experienced the greatest change over time, those that contributed to the replacement of forests and marshes, evaluate for forest to marsh, marsh to forest, and forest to water transitions, and to understand the influence that elevation has on forest-marsh dynamics. I hypothesize that 1) landward migration rates of coastal marshes increased from the first-time interval to the second-time interval for both estuarine areas, and 2) these increases were larger in GBNERR due to higher salinity than in Pascagoula.

1.2 Methods

1.2.1 Study Sites

The GBNERR and Pascagoula estuaries are both located in coastal Mississippi, less than 20 km apart, have microtidal diurnal tidal regimes, identical subtropical climates, similar geomorphological properties, a slope of 1-1.5˚, and an average water depth of 0.6-0.9 m (Christmas, 1973; Peterson et al., 2007; Wu et al., 2020). These similarities make them ideal for comparison. GBNERR and Pascagoula represent 15% and 35% of the coastal wetland area in Mississippi, respectively, see Figure 1.1 (Wu et al., 2020). However, the GBNERR and Pascagoula estuaries represent two extremes when it comes to fresh water and fluvial sediment inputs.

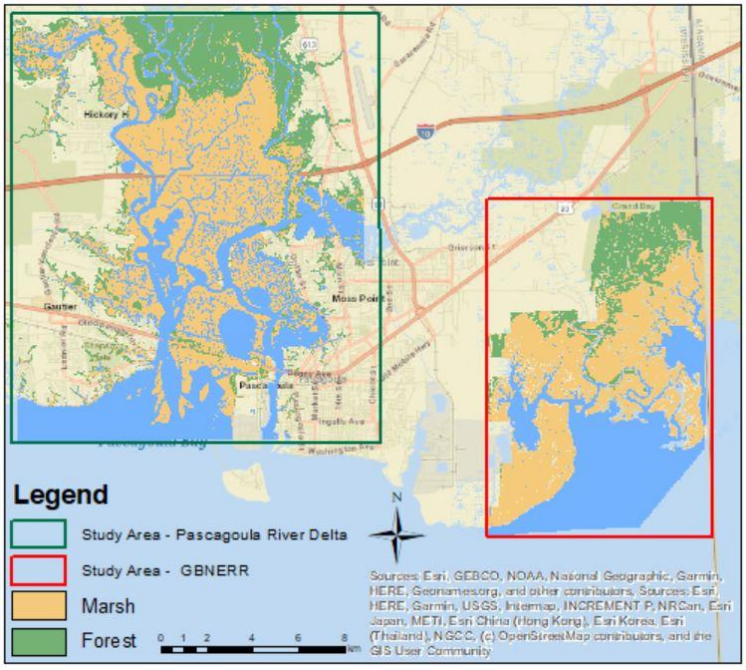

Figure 1.1 *Map depicting the studies areas of the Pascagoula River delta and the Grand Bay National Estuarine Research Reserve*

Map from the Pascagoula River delta depicts land cover classifications for marsh and forest from 2014. Classifications were obtained from Waldron et al., 2021. The Grand Bay National Estuarine Research Reserve map depicts forest and marsh cover from 2015. Classifications were obtained from World View-3 courtesy of the Grand Bay National Estuarine Research Reserve staff.

GBNERR, which is located on the Mississippi/Alabama border, includes over 7200 ha within its boundary and is a marine dominated estuary (Grand Bay National Estuarine Research Reserve, 2013). GBNERR was the first National Estuarine Research Reserve to represent the Louisianian biogeographical region and a part of the Mississippi deltaic subregion (Peterson et al., 2007). The Escatawpa River, which was the primary sediment source for GBNERR, naturally diverted into the Pascagoula River- effectively cutting off GBNERR's sediment supply (Eleuterius and Criss, 1991). As GBNERR no longer has a fluvial sediment source it is now considered a retrograding delta; meaning that sediment inputs are less than what is lost through subsidence or erosion (Grand Bay National Estuarine Research Reserve, 2013). Freshwater inputs into the area consist of occasional run off from land as large volumes of freshwater do not regularly enter the system. Salinity measurements have been recorded above 30 ppt at all System-wide Monitoring Program Stations, making it one of the most saline estuaries on the Mississippi coast (Grand Bay National Estuarine Research Reserve, 2013). Marsh area at GBNERR is predominately made up of *Juncus roemerianus* with a narrow band of *Spartina alterniflora* near the water's edge where the salinity is higher (Wu et al., 2020).

The Pascagoula estuary is a riverine dominated estuary that contains natural marsh as well as altered shorelines, mostly in the eastern tributary (Partyka and Peterson, 2008). The Pascagoula River that feeds into this system is the largest undammed river, by volume, in the contiguous United States (Jackson, 2012; Wu et al., 2020; Waldron et al., 2021). This river had an average discharge of 11,520 ft^3/s from 1994-2009 (U.S. Geological Survey, 2016). With large freshwater inputs, this area has lower overall water salinity with greater species richness (Wu et al., 2020). However, *J. roemerianus* still

dominates the marsh areas with narrow bands of *S. alterniflora* at the water's edge (Wu et al. 2020; Waldron et al., 2021). Pascagoula receives a lot of fluvial sediment inputs, creating a more conducive environment for vertical accretion.

1.2.2 Data Used

A combination of aerial and satellite imagery was used for analysis. Imagery for GBNERR was obtained from the National Wetland Inventory (NWI) for the years 1955 and 1988 (obtained from Shirley and Battaglia, 2006), and WorldView-3 for 2015 (courtesy of GBNERR staff). For Pascagoula, aerial imagery was obtained from Waldron et al. (2021). The Pascagoula imagery used originated from the U.S. Geological Survey for 1955, the National Aerial Photography Program for 1996, and the National Agriculture Imagery Program for 2014.

2005 LiDAR-derived elevation was used to evaluate at what elevations transitions were occurring. The elevation data was collected by the Army Corp of Engineers and obtained from the National Oceanic and Atmospheric Association (NOAA) (https://coast.noaa.gov/dataviewer).

1.2.3 Land Cover Classifications and Data Preparation

The land cover classifications were maintained from the original studies. For Shirley and Battaglia (2006), GBNERR classifications were based on the Cowardin et al. (1979) classification system and the uplands were classified based on a custom system by Anderson et al. (1976). The 2015 land cover classifications were created by segmentation in eCognition (J. Pitchford, personal communication, March 31, 2022). For the purposes of this study, similar land cover classifications were combined. For example, low marsh, mid marsh, and high marsh were combined into the single classification "marsh."

Waldron et al. (2021) created the Pascagoula land cover classifications based on a maximum likelihood classification scheme using spectral and textural image features. This study created four classifications which included: woodland, marsh, unvegetated, and water. These classifications were maintained with no alteration for this study. For constancy, woodland will be henceforth referred to as forest and unvegetated referred to as non-vegetated.

As GBNERR had data that came from two different sources, in order to ensure that the areas were the same resolution; the 2015 imagery which was originally 1.2x1.2 m was resampled so that the pixel size matched that of the 2x2 m resolution for the 1955 and 1988 images. The images were then clipped to match of that of the GBNERR boundary. As all classified maps for Pascagoula were provided by the same source, resampling was an unnecessary step. A total of 7247.32 and 11485.61 ha were analyzed for GBNERR and Pascagoula, respectively.

1.2.4 Analysis

I applied the Land Change Modeler in TerrSet 2020 to evaluate the land cover changes for Pascagoula and GBNERR. The Land Change Modeler allows for rapid assessment of land cover change between two maps and shows both maps and graphs of gains and losses of land cover types, net changes, and transitions from one specific type to another (Eastman, 1987). I compared 1955 to 1988 (first-time interval) and 1988 to 2015 (second-time interval) for GBNERR and 1955 to 1996 (first-time interval) and 1996 to 2014 (second-time interval) for Pascagoula. I assessed overall net changes and then evaluated based on areas where forest transitioned to marsh, marsh transitioned to forest, and marsh transitioned to water. The amount of area in ha that changed was determined

based on the count of the number of cells for a given land cover type in ArcMap 10.8.1 and area of each cell.

In order to evaluate at what elevations the transitions were occurring, I overlayed the rasters with the 2005 elevation data and clipped them to the extent of the 2005 elevation raster. I assume elevation of 2005 represents average elevation for the second time intervals (1988 to 2015 for GBNERR and 1996 to 2014 for Pascagoula). I grouped elevation data based on the current tidal elevation specific to each study area. These categories included mean low water level (MLW) and below, MLW to mean tidal level (MTL), MTL to mean high water level (MHW), and MHW and above. Elevations for each water level was based on data reported by NOAA using station #8740166 for GBNERR located at 30° 24.8 N, 88° 24.2 W with an epoch of 1983-2001 and station #8741533 for Pascagoula located at 30° 22.1 N and 88° 33.8 W with an epoch of 1983 - 2001. Table 1.1 shows the elevation ranges for each of these different water levels. Water levels were described as current due to not having data on the tidal levels that spanned the first time periods.

Table 1.1 *Elevation ranges corresponding to current water levels for GBNERR and Pascagoula*

MLW= mean low water level, MTL = mean tidal level, MHW = mean high water level, NAVD = National American Vertical Datum

Current Water Level Range	Grand Bay NERR Elevation Range (m, NAVD88)	Pascagoula Delta Elevation Range (m, NAVD88)
< MLW	-0.710 to -0.144	-1.250 to -0.174
MLW-MTL	-0.144 to 0.065	-0.174 to -0.033
MTL-MHW	0.065 to 0.273	0.033 to 0.239
>MHW	0.273 to 25.610	0.239 to 21.230

Based on those elevation ranges, zonal histograms were created in order to analyze where the forest to marsh, marsh to forest, and marsh to water transitions were taking place. Rates at which areas transitioned from one habitat type to another were calculated. As I only had land cover maps for three different years at each area, rates of change were determined by taking the total area that transitioned from one year to the next available year and dividing it by the number of years in that time interval so 33 or 41 for the first-time interval and 27 or 18 for the second-time interval for GBNERR and Pascagoula, respectively. This will allow for comparison between the two study sites

1.3 Results

1.3.1 Summary

The dominant land cover types in 1955 at GBNERR were marsh, water, and agriculture. It is important to note that agriculture land included forest plantations and grazing fields here and therefore did not represent traditional croplands. See discussion for details. By 1988 the agriculture land cover type was no longer present at GBNERR and had largely transitioned to forest without intensive management. In 1988 and 2015 at GBNERR the three dominant land cover types were marsh, water, and forest. At Pascagoula the largest for all years was marsh followed by water and forest. During the first- and second-time intervals at GBNERR and the second-time interval at Pascagoula, the largest transition by area and rate was for marsh transitioning to water while at Pascagoula for the first-time interval it was for marsh transitioning to forest. The least amount of area with the lowest rate of change for both study sites was for forest transitioning to marsh. However, by percent of original land cover that transitioned, the greatest change is the percent of forest transitioning to marsh. The rate at which forest

transitioned increased greatly from the first-time interval to the second for both areas. The greatest percent and most of the areas where marsh transitioned to forest occurred at elevations of the current MHW or greater for GBNERR and Pascagoula. For both time intervals at GBNERR and the second-time interval at Pascagoula, the greatest percent of forest area that converted to marsh occurred at elevations between the current MTL and MHW. During the first time-interval at Pascagoula the greatest percent change occurred between the elevations of the current MLW- MTL. However, the largest areas of forest converting to marsh were occurring at elevations of the current MHW or greater.

1.3.2 Land Cover Changes

For GBNERR, I defined a total of 11 different land cover types (Table 1.2). The three dominant land cover types in 1955 were marsh, water, and agriculture with areas of 3869.72, 2380.07, and 698.91 ha, respectively. For 1988 and 2015 the three dominant land cover types were marsh, water, and forest with areas of 3625.12, 2572.34, and 896.62 and 3131.60, 2570.24, and 981.70 ha, respectively (Table 1.2). The largest transitions during the first-time period occurred from the gains in forest area and the loss of agriculture and marsh area. By 1988 the agriculture land cover classification was no longer present with all 698.91 ha having converted to other land cover types. This loss was primarily due to transition to forest with the majority of these transitions occurring in the northern part of the map (Figure 1.2). Forest during this time interval gained 852.8 ha. Marsh from 1955 - 1988 lost 234.6 ha.

From 1988-2015, the second-time interval at GBNERR, the largest transition occurred in the marsh land cover type with a net loss of 493.52 ha followed by non-

vegetated which had a net gain of 340.14 ha, and forest with a net gain of 85.08 ha (Table 1.2 and Figure 1.2).

Table 1.2 *Land cover types at GBNERR and the amount of area they occupy*

NA indicates that the land cover was not present at the given year.

Cover Type	1955 area (ha)	1988 area (ha)	2015 area (ha)
Marsh	3859.72	3625.12	3131.60
Water	2380.07	2572.34	2570.24
Agriculture	698.91	NA	NA
Upland vegetation	219.66	54.27	56.62
Forest	43.82	896.62	981.70
Non-vegetated	13.51	78.82	418.96
Impervious	10.16	19.76	3.97
Freshwater marsh	NA	NA	43.99
Marsh/shrub	NA	NA	9.048
Salt pan	NA	NA	31.19
Modified vegetation	NA	0.68	NA

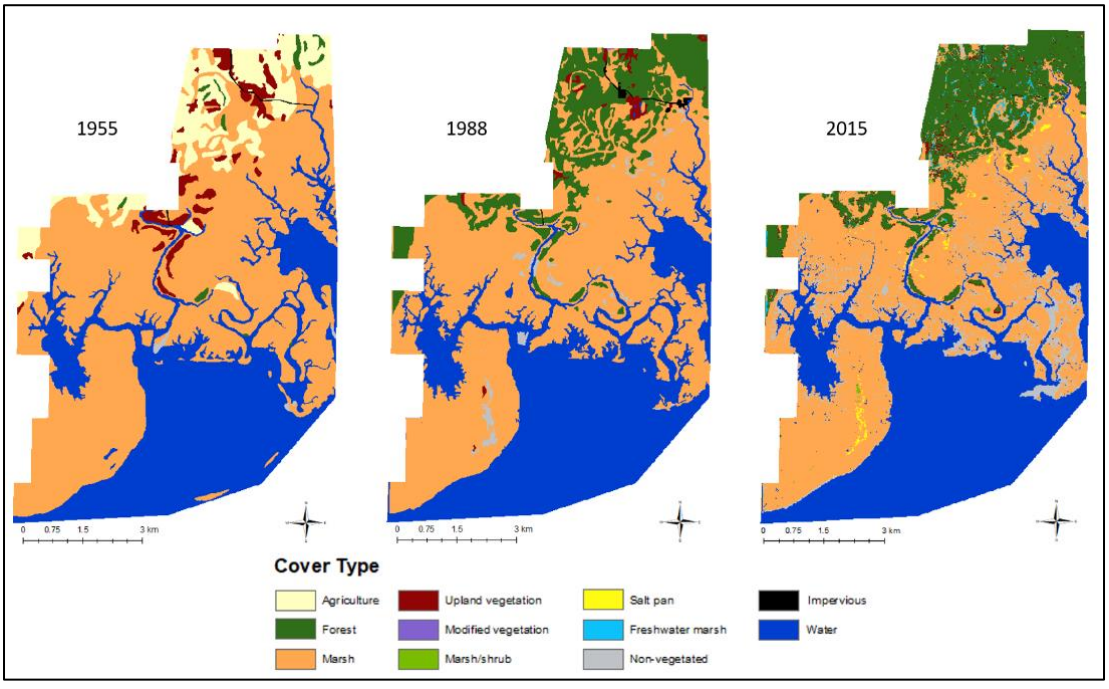

Figure 1.2 *Land cover classifications for 1955, 1988, and 2015 at GBNERR*

For all years at Pascagoula, the largest land cover type was marsh followed by water, forest, and non-vegetated (Table 1.3). The greatest change that occurred during the first-time frame was a net loss of marsh area with 767.30 ha, followed by a net gain by forest with 366.16 ha. The gains by forest primarily occurred in the northern part of the map (Figure 1.3). During the second-time frame, the greatest change occurred in the marsh area with a net loss of 294.98 ha followed by water with a net gain of 267.35 ha.

Table 1.3 *Land cover types at Pascagoula and the amount of area they occupy*

Cover Type	1955 area (ha)	1996 area (ha)	2014 area (ha)
Marsh	6116.07	5348.80	5053.82
Water	3325.09	3660.38	3927.73
Forest	1648.88	2015.04	2170.38
Non-vegetated	397.75	459.79	333.68

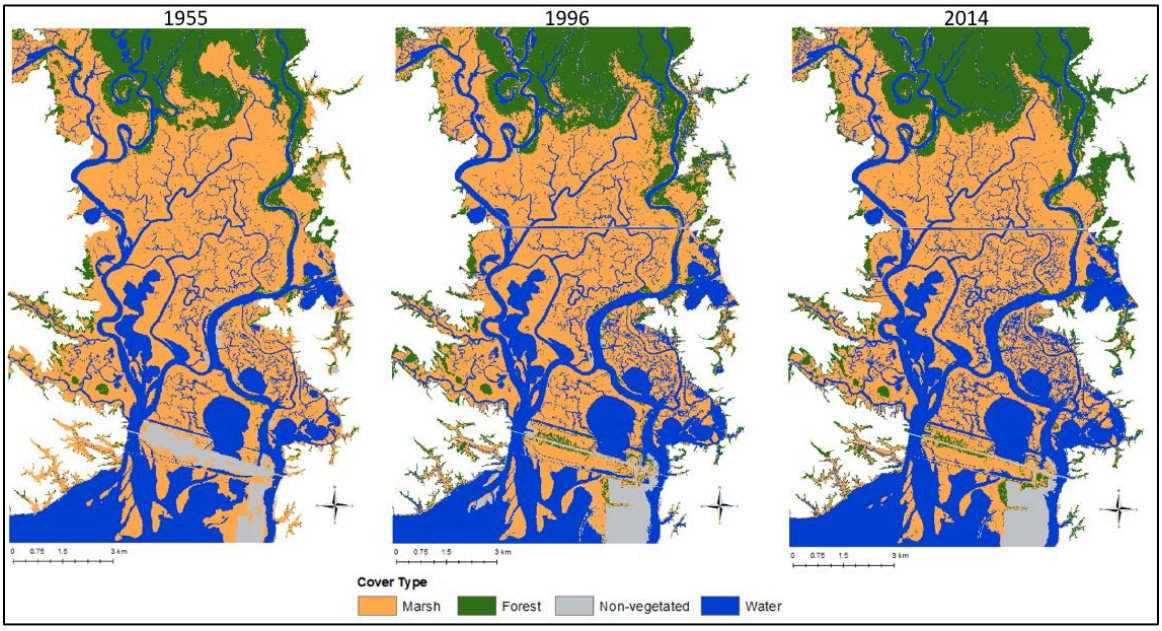

Figure 1.3 *Land cover classifications for 1955, 1996, and 2014 at Pascagoula*

1.3.3 Transitions of Forest to Marsh, Marsh to Forest, and Marsh to Water

By area and rate (ha/year), the largest transition that occurred at GBNERR during the first-time interval was for marsh transitioning to water. A total of 327.43 ha of marsh converted to water at a rate of 9.92 ha/year. During the first-time interval at Pascagoula, marsh converting to forest was the largest transition with 603.64 ha transitioning during that time frame at a rate of 14.72 ha/year (Table 1.4). For both study areas and time intervals, the least amount of area that transitioned was for forest transitioning to marsh. During the first-time interval 9.24 and 205.91 ha converted to marsh at a rate of 0.28 and 5.02 ha/year for GBNERR and Pascagoula, respectively. For GBNERR this was significantly less than the area transitioning from marsh to forest. However, in 1955 there was only 43.82 ha of forest so area that transitioned from forest to marsh made up 21.09 % of the total forest area. While the only 5.11% of the total marsh area in 1955 converted to forest and 13.59% of the marsh area converted to either water or forest (Table 1.4 and Figure 1.4). While Pascagoula had a similar trend with a greater percent of forest area that transitioned to marsh (12.49%) than percent of marsh that transitioned to forest (9.87%), there was a larger percent of marsh transitioning to forest or water (18.1%) than percent of forest converting marsh, differing from GBNERR.

The second-time interval at GNRERR and Pascagoula followed the same trend where the largest area that transitioned was for marsh converting to water (188.23 and 356.23 ha, respectively), followed by marsh transitioning to forest (179.36 and 331.95 ha, respectively), and forest transitioning to marsh (83.59 and 231.81 ha, respectively). The highest rates of change for both areas in the second-time interval was for marsh

transitioning water while the greatest percent of original land cover that transitioned for both study areas was for forest transitioning to marsh (Table 1.4).

From the first-time period to the second at GBNERR, percent of the original land cover type that transitioned as well as the rate at which it transitioned decreased for marsh transitioning to water going from a rate of 9.92 ha/year to 6.97 ha/year and going from 8.48% of the marsh transitioning in 1955 to 5.19% of the marsh transitioning from 1988 (Table 1.4). The percent of marsh area that transitioned to forest also declined from the first-time interval to the second going from 5.11% to 4.95%. However, there was an increase in the rate at which the marsh transitioned to forest moving from 5.98 ha/year to 6.64 ha/year (Table 1.4). This trend was also observed at Pascagoula with an increase of 3.72 ha/year from the first-time interval (14.72 ha/year) to the second (18.44 ha/year) converting from marsh to forest, but a decrease of 3.66% in the area of marsh that transitioned to forest (Table 1.4). Additionally, there was a large increase in the area that transitioned from forest to marsh going from the first-time interval to the second as well as in the rate at which it transitioned. The area that transitioned from forest to marsh at GBNERR was increased to 83.58 ha and the rate increased by 1007.1% to 3.1 ha/year (Table 1.4). This trend was also observed at Pascagoula but to a lesser extent; forest area that transitioned to marsh increased by 25.9 ha from the first-time interval. The rate also increased by 156.6 % from the first-time interval to the second (Table 1.4). However, the percent of forest area that transitioned to marsh decreased for both study areas from the first-time interval to the second. Pascagoula from the first-time interval to the second saw an increase of 7.51 ha/year for marsh transitioning to water yet 1.56% decrease in the percent area of marsh that converted to water (Table 1.4).

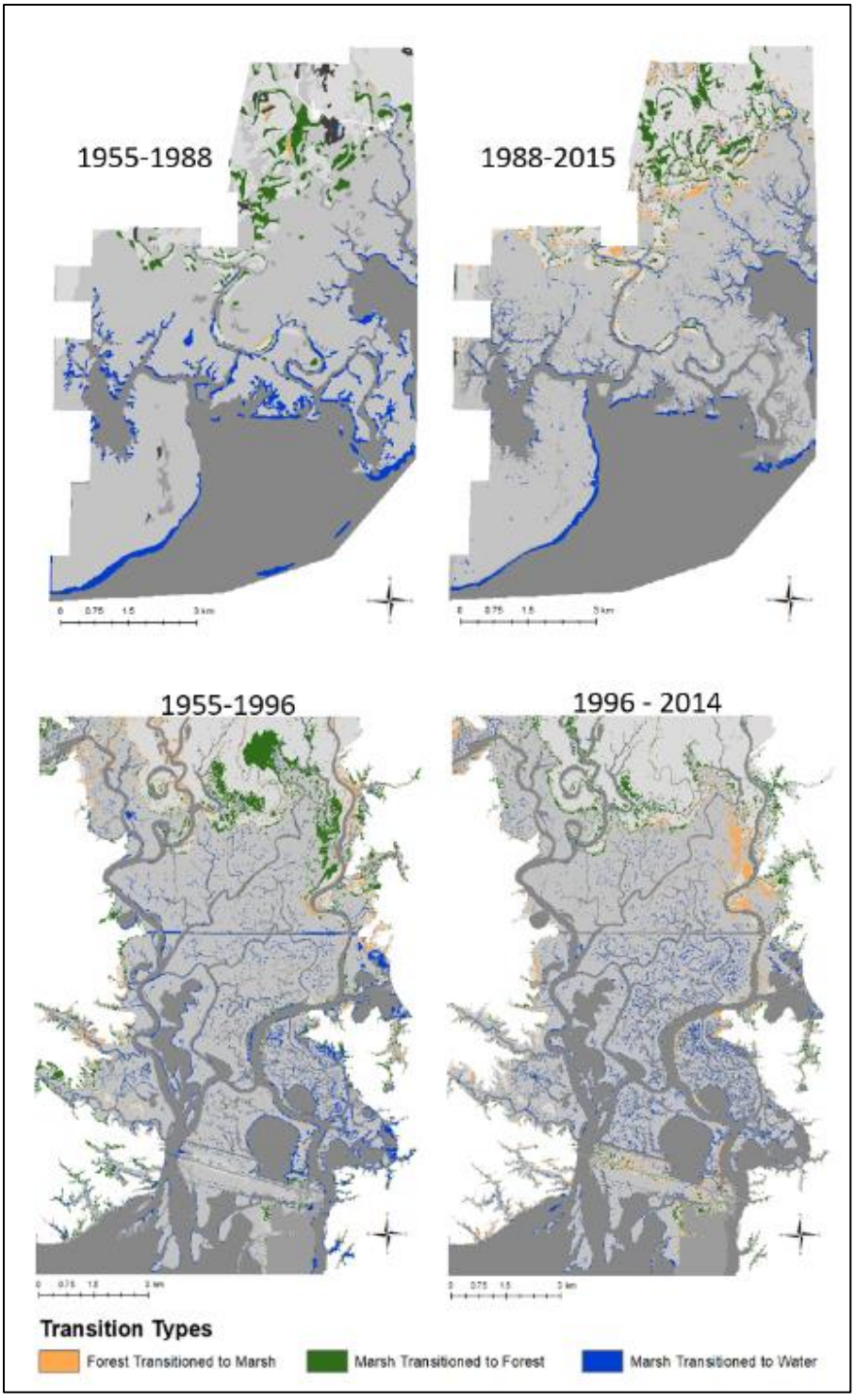

Figure 1.4 *Areas where the forest to marsh (yellow), marsh to forest (green), and marsh to water (blue) transitions occurred at GBNERR (top row) and Pascagoula (bottom row) during the first- (left column) and second-time interval (right column)*

Table 1.4 *Rates in ha/year for transitions of forest to marsh, marsh to forest, and marsh to water occurred at GBNERR and Pascagoula as well as the percent of original land cover that transitioned*

Transition	GBNERR 1955 - 1988	GBNERR 1988 - 2015	Pascagoula 1955 - 1996	Pascagoula 1996 - 2014
Marsh to forest (ha/year)	5.98	6.64	14.72	18.44
Marsh to forest (%)	5.11	4.95	9.87	6.21
Forest to marsh (ha/year)	0.28	3.10	5.02	12.88
Forest to marsh (%)	21.09	9.32	12.49	11.50
Marsh to water (ha/year)	9.92	6.97	12.28	19.79
Marsh to water (%)	8.48	5.19	8.23	6.67

1.3.4 Influence of Elevation on Forest-Marsh Dynamics

Data was compared to the 2005 elevation data. Totals may not match that of previous results because the analysis could only be done for areas where there was elevation data.

Looking at forest-marsh dynamics with relation to elevation, I found that the majority of the marsh area that transitioned to forest occurred at elevations at or above the current MHW for both study areas and time intervals. These areas also had the greatest rates of change (Table 1.5). At this elevation range, 2.3% and 1.3% of the marsh area transitioned to forest at GBNERR and 13.2% and 8.3% at Pascagoula for the first- and second-time interval, respectively (Figure 1.5). There are much higher rates of transition occurring at Pascagoula than at GBNERR.

The greatest percent change for forest transitioning to marsh occurred at elevations between the current MTL and MHW for both time intervals at GBNERR (48.1% and 65.1%, respectively) and the second-time interval at Pascagoula (42.9%). While for the first-time interval at Pascagoula the greatest percent change occurred between elevations of the current MLW and MTL (Table 1.6 and Figure 1.5). However, the highest rates of change in ha/year were occurring at the current MHW and above for GBNERR for both time intervals as well as Pascagoula during the first-time interval. For the second-time interval at Pascagoula, the highest rates of change were occurring between the current MTL and MHW (Table 1.6). Pascagoula had higher rates of change than GBNERR except for the second-time interval at elevations of the current MHW and above.

Table 1.5 *Rates at which marsh transitioned to forest by current tidal elevations at GBNERR and Pascagoula during the first- and second-time interval*

Bolded lines represent where the greatest precent change was occurring for each time interval and study area corresponding to Figure 1.5. <0.01 shows that there was some change that occurred with rates greater than 0 but changes were minimal.

Elevation Range	GBNERR		Pascagoula	
	Marsh to Forest 55-88 (ha/year)	Marsh to Forest 88-15 (ha/year)	Marsh to Forest 55-96 (ha/year)	Marsh to Forest 96-14 (ha/year)
	1955 Marsh area (ha)	1988 Marsh area (ha)	1955 Marsh area (ha)	1996 Marsh area (ha)
< MLW	0.00	0.00	0.02	0.01
	83.33	60.98	52.70	25.56
MLW- MTL	< 0.01	< 0.01	0.12	0.09
	72.71	66.20	206.00	149.50
MTL-MHW	0.02	<0.01	0.34	0.36
	255.49	213.40	740.41	712.60
> MHW	**1.20**	**0.86**	**7.35**	**9.46**
	1750.65	**1766.26**	**2281.93**	**2048.65**

Table 1.6 *Rates at which forest transitioned to marsh by current tidal elevations at GBNERR and Pascagoula during the first- and second-time interval*

Bolded lines represent where the greatest precent change was occurring for each time interval and study area corresponding to Figure 1.5. <0.01 shows that there was some change that occurred with rates greater than 0 but changes were minimal.

Elevation Range by Current Water Level	GBNERR		Pascagoula	
	Forest to Marsh 55-88 (ha/year)	Forest to Marsh 88-15 (ha/year)	Forest to Marsh 55-96 (ha/year)	Forest to Marsh 96-14 (ha/year)
	1955 Forest area (ha)	1988 Forest area (ha)	1955 Forest area (ha)	1996 Forest area (ha)
< MLW	<0.01	0	0.01	0.02
	0.23	<0.01	2.12	1.71
MLW-MTL	<0.01	<0.01	**0.11**	0.18
	0.05	0.09	**11.25**	8.68
MTL-MHW	**<0.01**	**0.03**	0.24	**0.62**
	0.09	**1.10**	26.12	**25.99**
> MHW	0.08	1.02	2.29	0.15
	9.53	160.64	816.51	1024.794

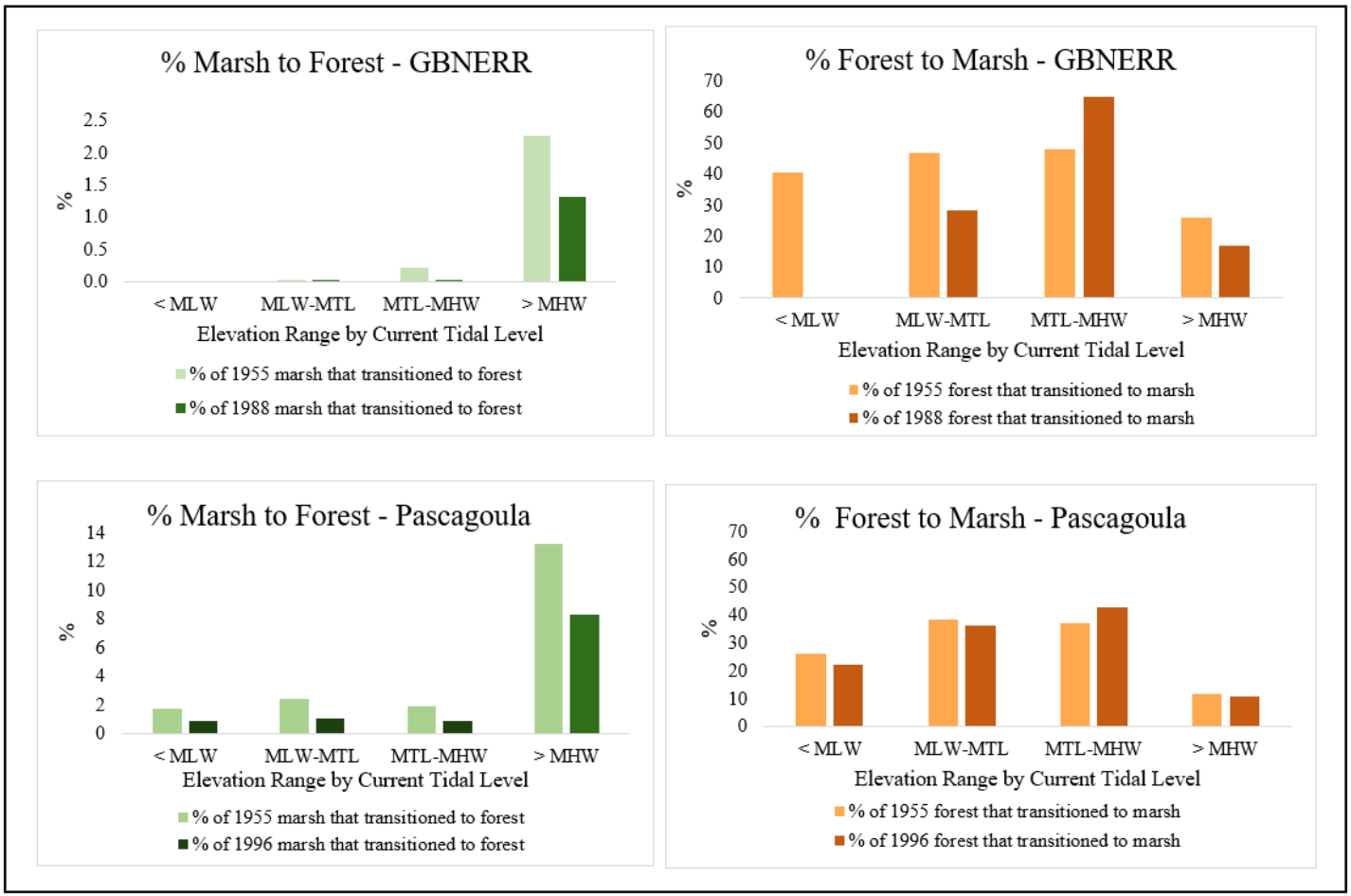

Figure 1.5 *Percent of original cover type that transitioned by current tidal elevation and time interval for GBNERR and Pascagoula*

1.4 Discussion

Looking at the transitions between all land cover types at GBNERR, the greatest change that occurred during the first-time interval was from loss of agriculture which primarily transitioned to forest by 1988. It is important to note that the agriculture land cover classification was a broad term that included forested plantations and is therefore distinct from traditional croplands. During this time, GBNERR had pecan orchards and potentially some citrus - although much of the citrus orchards had been killed during a deep freeze in the 1940s (Wieland et al. 1998; Peterson et al. 2007). The agriculture land cover type is likely misrepresenting areas that should have been classified into forest and because of this the forest land cover type during 1955 was likely larger than orginally represented. In addition, agriculture also included grazing. By the late 1920s much of the large timber had been harvested and pecans did not bring in enough profits, so the open treeless land was used for free-range grazing of large sheep herds and cattle until a 1956 anti-free range law was passed (Wieland et al., 1998). After which livestock could only graze in penned areas. Again agriculture acted as a large catch-all and misrepesented the actual land use during 1955. The second-time frame was characterized by a large loss of marsh area which contibuted to gains in forest and non-vegetated cover types. The loss in marsh area was the largest land cover change for both time intervals at Pascagoula. The losses of which contributed to gains in water and forest areas. Marsh transitioning to forest may be attributed to a lack of fire. Fire management of forest area is used to clear understory vegetation in order to create and maintain an open canopy to support diversity and prevent hardwood and shrub species from establishing themselves. In the absence of

fire the understory can become highly shaded which makes it difficult for high marsh grass species such as *Spartina patens* to outcompete the upland vegetation (Brinson et al., 1995).

I found that while there was replacement of forest by marshes there was greater loss, by area, of marshes transitioning to forest and water at both sites. These findings are supported by Shirley and Battaglia (2006) and Waldron et al. (2021). Hillbert (2006) also found the land cover change at GBNERR was largly characterized by loss of wetlands to open water from 1974-2001. While there is evidence for landward migration of marshes at both GBNERR and Pascagoula, those gaines were much smaller than losses at the water's edge. These results differ from a study of the Chesapeake Bay that found that loss of marshes to shoreline erosion was offset by marsh area that was created by upland drowning (Schieder et al., 2018). Additionally, loss of marshes at the shoreline was found to be offset by marsh expansion into forested area in the Big Bend region of Coastal Florida (Raabe and Stumpf, 2016). However, these studies looked at a much longer periods of land cover change of over 100 years. Linscombe and Hartley (2011) found that there was a decrease in wetland area along coastal Louisiana from 1978-2001 with wetland converting to open water. Marsh decline is influenced by many variables such as sediment availability, slope, and vegetation among other environmental factors so rates may vary largely from one area to another (Kirwan et al., 2010; Waldron et al., 2021).

When looking at percent changes of forest area transitioning to marsh, these occurred prodominently at elevations between the current MTL and MHW. This may be due to a salinity maxium that can occur at MHW. Areas at these higher elevations are

inundated less frequently allowing for greater evapotranspiration which can cause salt to accumulate in the soil. Wang et al. (2007) found that the salinity maxiumum in a semi-diurnal mash was driven by mean higher high water but in a diurnal tidal regime MHW would determine the location of the maxium. Due to the salinity maximum it is likely that the glycophytic upland vegetation becomes too stressed allowing the halophytic marsh vegetation to out compete and occupy the area. Kirwan et al. (2007) found that salinity stress can impact recruitment of new trees. Additionally, at the lowest elevations there is very little forest area to begin with due to high salinity stress and frequent inundation which is likely why there is so little change occurring at elevations less than the current MTL.

The highest rates and greatest percent of marsh transitioning to forest for both study sites and all intervals was occurring at elevations of the current MHW and above. This is likely due to less salinity stress at higher elevations-allowing glycophtyes such as *Spartina patens, Cladium maricus, Baccharis halimifolia, Panicum virgatum,* and upland tree species such as *Pinus elliotti* to outcompete and establish themselves as opposed to the more salt tolerant *J. romerianus* (Battaglia et al., 2012).

This reseach can help managers understand the land cover changes occurring at GBNERR and Pascagoula. However, due to the inherent differences on how the imagery was classified and contraints on the imagery available, I would caution against using this data as the sole basis of comparision between the two study areas. This analysis could be more robust if more imagery were obtained and comparison would more feasible if images were of the same year and the same type. Additionally, perscibed fire has long

been used as a tool to manage forested area, and is used today at GBNERR in the pine savannas (Grand Bay National Estuarine Research Reserve, 2013). Fire can have impacts on habitat availability as well as altering the hydrological cycle. It would be beneficial to evaluate the impacts of fire management on landward migration using imagery from before and after fire events. This research paired with the results found in Chapter 2, will ultimately be used to facilitate the development of a mechanistic model that will predict the landward migration of salt marshes. These results on historical land cover change will be used to calibrate the mechanistic model.

1.5 Conclusion

I found that there are larger areas of marsh that are transitioning to forest and these transitions are primarily occurring at higher elevations. The greatest percent change of marsh transitioning to forest is primarily occurring at elevations of the current MHW and above. However, for GBNERR the rate at which the transitions were occurring at these elevations did decrease from the first-time interval to the second. The greatest percent changes are occurring for forest to marsh transitions and between the current MLW and MHW. The areas of forest that transitioned to marsh increased from the first-time interval to the second for both study sites (Hypothesis 1), but was more pronounced at GBNERR (Hypothesis 2). Finally, while there is landward migration of coastal marshes into the forest area, it cannot keep up with amount of marsh area that is lost to water or forest in either time interval for either study site.

CHAPTER II –THE IMPACTS OF SOIL POREWATER SALINITY AND FIRE MANAGEMENT ON THE MARSH, ECOTONE, AND FOREST HABITATS

2.1 Introduction

The Northern Gulf of Mexico (NGOM) is characterized by gradually sloping coastal areas which are conducive to large salinity gradients (Battaglia et al., 2012). Higher soil porewater salinities are found at lower elevations by the seaward edge (Battaglia et al., 2012). Here, the porewater salinity is largely influenced by the incoming tide. As elevation increases into the upland area, the porewater salinity generally decreases due to lack of inundation. The salinity gradient created from tidal inundation and elevation is the driving force of the vegetation zonation of coastal wetlands (Eleuterius and Eleuterius, 1979).

The Grand Bay National Estuarine Research Reserve (GBNERR) is one of the most saline estuaries along the MS coast with over 30 ppt having been recorded at all of the System-wide Monitoring Program Stations (Grand Bay National Estuarine Research Reserve, 2013). There is limited freshwater input into GBNERR as the main source of freshwater, the Escatawpa River, naturally diverted into a tributary of the Pascagoula River (Eleuterius and Criss, 1991). Salinity values in the southern areas closer to the seaward edge range from 10-30 ppt while inland areas can vary between close to 0 to 25 ppt (Peterson et al., 2007). Salinity measurements are generally highest during the dry season in summer and early fall and lowest during the wet season in winter and spring (Grand Bay National Estuarine Research Reserve, 2013).

GBNERR has a very distinct vegetation zonation due to the porewater salinity and elevation gradients (Figure 2.1). Generally, there is a narrow band of *Spartina*

alterniflora at the fringe where the marsh area meets the water (Wu et al., 2020). The mid-marsh at GBNERR is dominated by monoculture-stands of *Juncus roemerianus* (Battaglia et al., 2012). Following the large mid-marsh area, is the high marsh which is predominantly *Spartina patens* and includes other species such as *J. roemerianus, Panicum virgatum,* and *Andropogon glomerates* as well as shrubs such as *Baccharis halimifolia* and *Iva frutescens* (Peterson et al., 2007). The ecotone area, which is between the high marsh and the pine savanna, is a narrow band of estuarine shrubland which includes *B. halimifolia, I. frutescens and Myrica ceriferia*. In the upland, is the maritime pine flatwood where *Pinus elliotii* is the dominate tree species with *S. patens* making up the understory (Peterson et al., 2007; Battaglia et al., 2012). Species also found in this area includes *P. virgatum, Cladium mariscus, Cynanchum angustifolium, Dichanthelium scabriusculum, B. halimifolia, Ilex vomitoria,* and *M. cerifera* (Peterson et al., 2007). As salinity stress decreases and elevation increases, biodiversity also increases going from monocultures such as *Juncus* to the more diverse areas of the slash pine savannas.

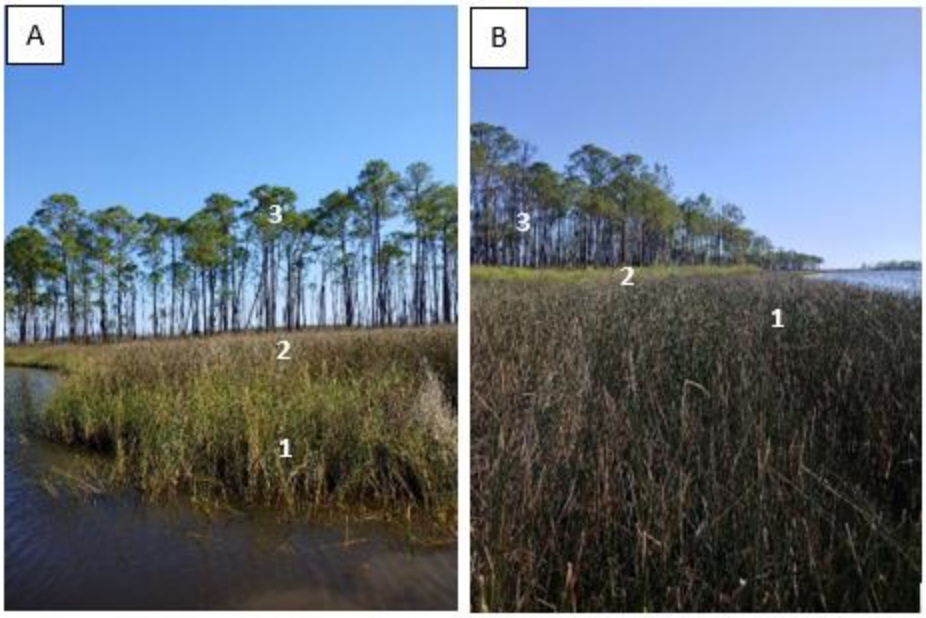

Figure 2.1 *Typical marsh zonation at the GBNERR*

Picture A is a frontal picture of marsh zonation at GBNERR depicting the narrow band of *S. alterniflora (1),* followed by *J. roemerianus (2)* in mid-marsh and upland forest dominated by *P. elliotii* (3). Picture B representing a cross section depicting the marsh (1), followed by the ecotone (2), and forest (3).

Increased inundation can raise the salinity of the porewater causing greater salinity stress at the forest-marsh edge (Brinson et al., 1995). This salinity stress can cause a die off of trees, creating ghost forests which are areas of snags and stumps surrounded by areas of salt marsh, and opening habitat for marshes to migrate landward or transgress (Kirwan and Gedan, 2019; Sacatelli et al., 2020). A study done by Raabe and Stumpf (2016) along the Gulf Coast of Florida, found that from the late 18th to the late 19th century, 82 km^2 of forested area had converted to marshland and an additional 66 km^2 of forest had converted to forest-marsh transitional habitat. Increased inundation may also limit recruitment of the forest (Kirwan et al., 2007). A Kirwan et al. (2007) study suggests that forest may retreat stepwise due to a decreased ability of forests to recruit, not as a result of mortality of mature trees due to increased porewater salinity.

Ecotones are typically narrow transitional areas between adjacent habitat types and can be sensitive indicators of climate change as the vegetation there is already on the periphery of their ranges/tolerances (Risser, 1995). Increased inundation and porewater salinity in these areas can cause the ecotone to migrate upland or potentially convert to the more salinity tolerant marsh vegetation (Wasson et al., 2013; Elsey-Quirk et al., 2019).

How the landscape changes will largely be influenced by how SLR will alter the hydrological cycle. Wang et al. (2007) found that the highest porewater salinities were not at the water's edge but occurred at a band driven by the higher high water level. This is due to evapotranspiration (ET). At the lower elevations the porewater salinity will be close to that of the tide. The closeness in salinity occurs because these areas are less impacted by ET as they are inundated frequently. At elevations of higher high water or high water in a diurnal system, tidal inundation is less frequent allowing for ET of water. The ET of the water causes salt to accumulate in the soil, creating high saline or even hypersaline areas (Hsieh, 2004; Wang et al., 2007). As SLR occurs and tidal inundation moves further up the elevation gradient, the maximum salinity band may move landward driving the change in plant communities.

The goals of this chapter are to 1) predict how soil porewater salinity changes under different SLR scenarios, 2) evaluate how vegetation responded to elevation and porewater salinity along the gradients of salt marsh-ecotone-pine savanna (forest), and 3) evaluate whether prescribed fire had any impact on vegetation or its response to elevation and porewater salinity. I have four specific objectives: 1) calibrate a simulation model by Wang et al., 2007 that will predict porewater salinity for every 0.05 m increase in

elevation for the marsh area by 2050 and 2100 under different sea level rise scenarios, 2) determine the relation between porewater salinity and elevation to above- and belowground biomass of salt marsh vegetation and understory vegetation of the ecotone and forest, and diameter at breast height (DBH) and height of slash pines in the ecotone and forest, 3) determine the impact of porewater salinity and elevation on change in DBH as well as change in height of slash pines, and 4) evaluate difference of vegetation and its response to elevation and porewater salinity between prescribed fire impacted sites and control sites. The results of this work will help predict how sea-level rise derived changes of elevation and porewater salinity, combined with prescribed fire management, affect vegetation biomass and structure in the future, and therefore facilitate the development of a marsh transgression model.

2.2 Methods

The study area is the GBNERR. Please refer to Chapter 1 for the detailed description of the study area.

2.2.1 Field Experiment Design

Originally, I planned to set up three transects, one transect in an area where a prescribed fire occurred in April of 2018, and the other two in areas free of fire impact - acting as controls. Due to the closure of federal lands caused by the pandemic in 2020, I only set up two transects on the state lands during the 2020 field season, one (Transect 2) acting as a control and one (Transect 1) with fire impact. The last prescribed fire occurred in 2018 at Transect 1. I added the third transect (Transect 3), serving as the second control transect, during the 2021 field season when federal lands reopened. Each transect was ~50 m long and spanned the forest, ecotone, and marsh habitats. There were a total

of 7 sites along each transect with 2 in the marsh, 3 in the ecotone, and 2 in the forest. Each site then consisted of three 5x5 m subsites with each subsite ~10 m from its neighbor. See Figure 2.2 for the setup of sites along the transect.

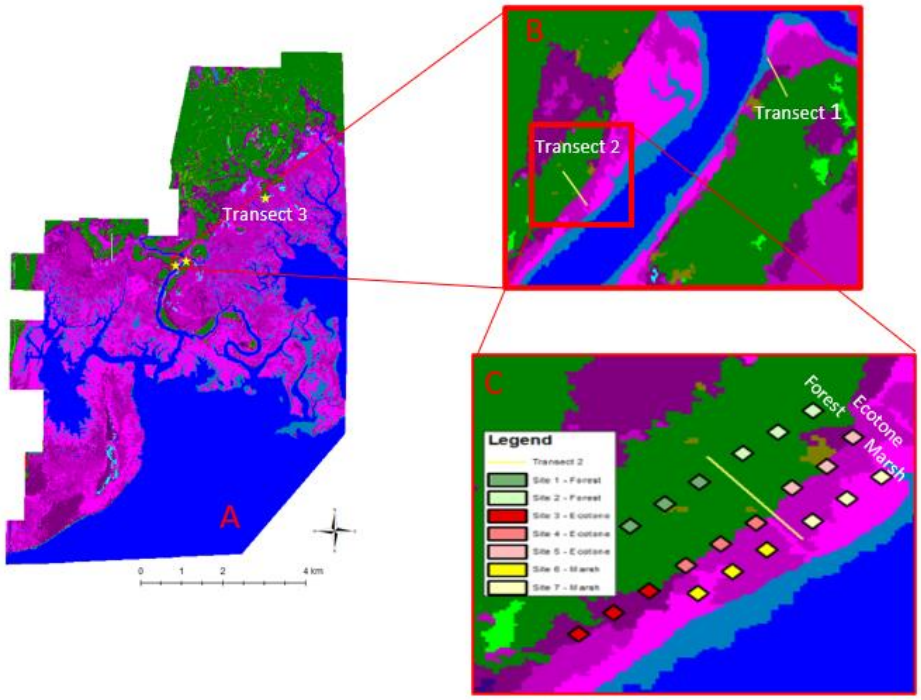

Figure 2.2 *Set up of field sites at GBNERR*

Map shows the setup of transects with A) showing all GBNERR with transect locations indicated by stars, B) showing Transects 1 and 2, and C) showing how sites were placed along the transect in the forest, marsh, and ecotone habitats

2.2.2 Field Collection

Any slash pines that grew within a subsite were marked by numbers starting with one and going up consecutively using aluminum, waterproof tree ID tags. Tags were attached using rope and tied so that the rope was not tight enough to impede growth. For each tree, measurements were taken for DBH and tree height. The first sampling event for tree data occurred between 2/8/2021-3/8/2021 which represented the status of trees at the end of growing season of 2020 assuming minimum growth during the winter, and the

second sampling event was completed between 7/20/2021- 8/5/2021 representing the status of trees during the peak growing season of 2021.

For tree heights, any trees that were over 11 feet were measured using a Haglöf Electric Clinometer which is ideal as heights can be measured from any distance or angle (Haglöf Inc.). Additionally, the clinometer uses the sine method, which produces the best results for trees that grow directly upward – making slash pines an ideal species. This method also produces less user error and lower random error (Larjavaara and Muller-Landau, 2013). In order to get the proper measurement, a measuring tape was used to get the exact distance from the base of the tree to eye level of the operator -where the clinometer was held. The input of distance from the clinometer determines the angle degree by aiming at the base of the tree and then the height by aiming at the tallest point of the tree. Two measurements were taken by two different observers and the results were averaged. Trees that were under 11 feet were measured using a PVC pipe marked in inches. One individual would hold the pole erect next to the tree and another, standing on a ladder, read the measurement of the tree height at eye level. Change in height and DBH were determined by taking the difference in measurements from the first sampling event to the second at Transect 1 and 2. As I had only 2021's measurements at Transect 2, there was no data of change in height and DBH at Transect 3.

Above- and belowground biomass samples of salt marsh vegetation and understory vegetation of the ecotones and pine savannas were collected within each subsite along the transects. Two 25x25 cm quadrats were randomly placed within the subsite, and all aboveground biomass from the sediment surface and above that was growing within the quadrats was collected. Once the aboveground biomass was collected,

a soil corer was used to remove the belowground biomass at the same location. The corer was 10 cm in diameter and 30 cm in length. Every soil core was separated into 5 cm-depth sections using a handsaw starting with the sediment surface until 30 cm in depth was reached or the whole soil core was used, whichever came first. Two cores were taken from every subsite with one serving as a replicate. From each belowground biomass sample a ~25 gram aliquot was removed for determination of soil porewater salinity. The aliquots were stored at -18˚C until processed. Above- and belowground biomass samples were stored at 4˚C until processed.

2.2.3 Processing Samples

Aboveground biomass was sorted into labeled aluminum pans by lowest identifiable taxonomic level and whether the individual was live or dead. Determination of whether the vegetation was live or dead was based on the presence or absence of green coloration. Weights were taken on the wet biomass. Once sorted and weighed, the aboveground biomass was dried in an oven at 70˚C for at least 3 days until constant weight and then reweighed to obtain the dry weight.

Belowground biomass samples were rinsed using a 1 mm sieve to remove any inorganic material. Once rinsed, sediment samples were returned to their resealable bags and stored at 4˚C until processed. The rinsed sediment samples were processed by sorting into live and dead biomass based on coloration, turgidity, and buoyancy (Wu et al., 2020). For example, roots that were lighter in color, floating, and stiff would be considered live while roots that were dark in color, sinking, and flaccid would be considered dead. The sorted belowground biomass was then placed into labeled aluminum trays and wet weights were taken. As with aboveground biomass,

belowground biomass samples were dried in an oven at 70˚C for at least 3 days after which dry weights were taken. For this study, I looked at total above- and belowground biomass. Replicates for each subsite were averaged to obtain one value per subsite.

Soil porewater salinity analysis was done in accordance with protocols determined by Hsieh (2004). Samples for determination of soil porewater salinity were placed into labeled aluminum tins to obtain their wet weight and then dried in an oven at 70˚C for ~3 days after which dry weights were taken. The dried samples were then placed into plastic cups and 25 mL of distilled water were added. Soil was then mixed well, covered, and left to sit for at least 12 hours in order to allow the suspended sediments to settle. After the 12 hours, water was placed onto a salinity refractometer that had been previously calibrated (Figure 2.3). The refractometer reading was then recorded and put into mass balance equation (Eq. 1) to determine the soil porewater salinity. All porewater salinity measurements of a given subsite were averaged to obtain one value per subsite.

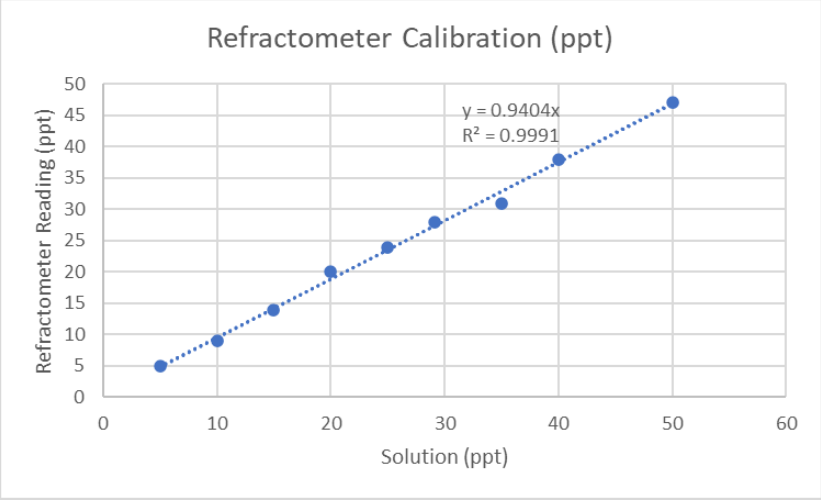

Figure 2.3 *Calibration of salinity refractometer*

Reading of the refractometer against a known stock solution.

$$Porewater\ salinity\ (ppt) = \frac{Measured\ salinity\ (ppt) \times 25\ ml}{Porewater\ volume\ (ml)}$$ - Eq. 1

Where the value of porewater volume is the same as the porewater weight in grams as the density of water is 1 g/ml, calculated as the different of wet sample weight and dry sample weight. Equation from Hsieh, 2004

2.2.4 Salinity Model

The porewater salinity simulation model that was used to predict porewater salinity by elevation for 2021 was from Wang et al., 2007. This model is based on the salt and water balance model from Morris (1995) but was adjusted in four ways. These include using the Penman-Monteith equation to calculate the daily evapotranspiration based on local climatic data, considering the impact of soil temperature on the saturated hydraulic conductivity, determining infiltration rate by comparing rainfall intensity and soil infiltration capacity, and setting the moisture level for closure of drainage (Wang et al., 2007). See Figure 2.4 for a flow chart of the model. The model then predicts soil porewater salinity for every 0.05 m in elevation for the marsh area.

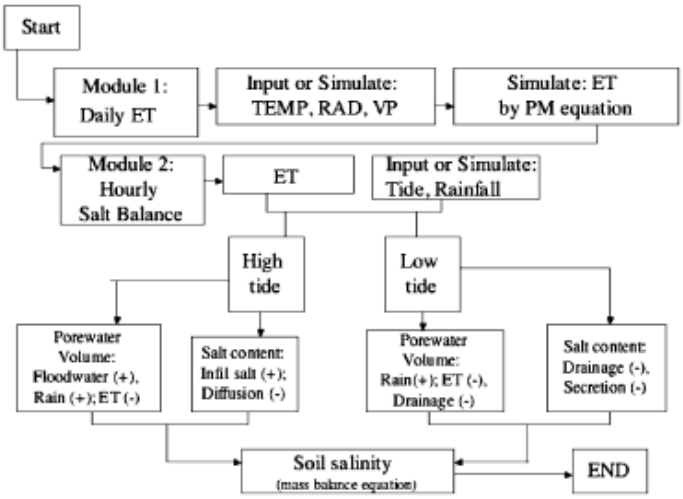

Figure 2.4 *Conceptual diagram of the salinity model*

Diagram is from Figure 1 of Wang et al., 2007

The model required input files for hourly precipitation (mm), daily air temperature (°C), hourly tidal elevation (NAVD88 m) and hourly salinity of incoming tide (ppt). All data was obtained from weather stations and tidal gauges located at GBNERR; with precipitation and air temperature from the Bureau of Land Management (BLM) in partnership with the Fish and Wildlife Service (FWS), tidal prediction from the National Atmospheric and Oceanic Administration (NOAA), and surface water salinity from the System-wide Monitoring Program at GBNERR. If data was collected at a more frequent interval, data was averaged to get the time interval needed (hourly or daily). See Table 2.1 for a summary of the input files and station information.

Missing data points for surface water salinity at the Bayou Cumbest station (closest to my transects) were derived using a regression equation between Bayou Cumbest and Bangs Lake data. The Bangs Lake station is also a part of the GBNEER's System-wide Monitoring Program and is the closest station to Bayou Cumbest. The linear regression used to derive missing data was $\hat{y}$= 1.16 (x) -7.32 with $\hat{y}$ representing the derived 2021 Bayou Cumbest salinity and x representing the 2021 Bangs Lake salinity data. The regression produced an R^2 of 0.8144. Missing air temperature data for the GRBM6 station was filled in using a linear regression between the 2021 GRBM6 data and 2020 Day Met data which had an R^2 of 0.479. The regression used was $\hat{y}$=0.73(x) + 4.59 with $\hat{y}$ representing the derived 2021 GRBM6 data and x representing the 2020 Day Met data. Additionally, from the GRBM6 station, if there was accumulated precipitation data missing and the amount of precipitation from the hour before to the hour after was the same, then that value would be copied into the missing cell as there was no additional

precipitation. If the hour prior and after were different, then the average of the two was used to fill in for the missing value.

Table 2.1 *Summary of input files for the salinity model*

BLM - Bureau of Land Management, FWS - Fish and Wildlife Service, NOAA - National Atmospheric and Oceanic Administration, GBNERR – Grand Bay National Estuarine Research Reserve

Data	Time Interval of Data Collection	Station Name	Location	Data Source
2021 Precipitation (mm)	Hourly	GRBM6	30.44°N 88.43°W	BLM and FWS
2021 Air Temperature (°C)	Hourly	GRBM6	30.44°N 88.43°W	BLM and FWS
2021 Tide Prediction (NAVD88 m)	Hourly	8740166	30.41°N 88.40°W	NOAA
2021 Surface Water Salinity (ppt)	15 minutes	Bayou Cumbest	30.38°N 88.44°W	GBNERR

I ran the model from January 1, 2021 to December 31, 2021 with daily outputs of simulated soil porewater salinity. However, as the model was calibrated to porewater salinity data that was collected on August 3, 2021, only August 3, 2021 was used. As the model can only be used to predict salinities for the marsh area, only marsh salinity was used for calibration. Only Transects 1 and 2 were used as they are closer together and Transect 3 marsh area is located on a salt panne and would overestimate soil porewater

salinity for the marsh area. A total of 10 points were used for calibration over elevations between 0.25 - 0.50 m (Table 2.2). If there were multiple points per elevational range the porewater salinity for measurements were averaged for calibration.

Table 2.2 *Soil porewater salinity for subsites within the marsh area used to calibrate the salinity model*

Elevation (m)	Point 1 (ppt)	Point 2 (ppt)	Point 3 (ppt)	Average Salinity (ppt)
0.25 ~ 0.30	22.85	NA	NA	22.85
0.30 ~ 0.35	20.18	24.88	21.79	22.28
0.35 ~ 0.40	21.47	23.75	NA	22.61
0.40 ~ 0.45	18.92	20.90	NA	19.91
0.45 ~ 0.50	22.26	NA	NA	22.26
0.50 ~ 0.55	20.54	NA	NA	20.54

Area specific soil information was used as the initial inputs for some important soil parameters and these parameters have been adjusted to make the model predicted soil porewater salinity as close to the measurements as possible. See Table 2.3 for the parameters' final values used based on the calibration.

Table 2.3 *Input values for different parameters of the salinity model*

*The basis for field capacity came from the Web Soil Survey for the axis mucky sandy clay loam with a reported field capacity of 0.236. However, based on model calibration I found this should be 0.56168 a 138% increase from that reported on Web Soil Survey and the minimum moisture should be 0.3068 a 30% increase from the reported 0.236 field capacity.

Parameters	Inputs for Calibrated Model	Source
Porosity (n)	**0.46**	Terrano (2018)
Ion Secretion Factor (k2)	**0.0**	No salt secretion by vegetation
Quotient of Transpiration/ET (k_3)	**0.5**	Morris (1995)
Salt Diffusion Coefficient (K_d)	**0.0725**	Morris (1995)
Field Capacity (Fc)	**0.56168**	Based on Web Soil Survey*
Wilting Point (wp)	**0.157**	Web Soil Survey
Hydraulic Conductivity (K)	**1.52**	Web Soil Survey
Initial Salinity	**12.0**	Average of salinity from GBNERR
Minimum Moisture	**0.3068**	Based on Web Soil Survey *
Bulk Surface Resistance to Water Vapor (rs)	**5.0**	Wang et al. (2007)
Aerodynamic Resistance (ra)	**2.0**	Wang et al. (2007)

Once the model was calibrated the tidal input file was adjusted to reflect the increase in sea level rise by 2050 and 2100. SLR scenarios chosen are based on the current rate of global mean SLR which is 3.6 mm/year (Wang et al., 2021), the current rate of relative sea level rise (RSLR) in Mississippi which is 4.68 mm/year as reported by NOAA (NOAA Tides and Currents), the threshold rate for marshes to be able to maintain themselves by 2100 at GBNERR determined to be 7.2 mm/year (Wu et al., 2020), and the observation-based extrapolation, low, intermediate-low, intermediate, intermediate-high, and high RSLR scenarios for the eastern gulf and the contiguous US for 2050 and 2100 reported in the USGS Global and Regional Sea Level Rise Scenarios for the United

States by Sweet et al. (2022). The amount of RSLR reported by Sweet et al. (2022) used a baseline of 2000, so the values were adjusted to reflect a baseline of 2021 which is what the model was calibrated to. This was done by dividing by either 50 or 100 for 2050 or 2100, respectively, in order to get the amount of SLR per year and then multiplied by either 29 or 79 to get the amount of SLR that would occur between 2021 and 2050 or 2100, respectively. Table 2.4 shows how the tidal input was adjusted for the 2050 scenarios and Table 2.5 shows how the tidal input was adjusted to reflect changes by 2100.

Table 2.4 *Amount added to tidal input to reflect SLR changes by 2050*

Source of values [a] = Wang et al., 2021, [b]= Wu et al., 2020, [c] = Sea Level Trends - NOAA Tides & Currents, [d]= Sweet et al., 2022.

Region	SLR Scenario	Increase amount with a baseline of 2000 (m)	Increase amount with a baseline of 2021 (m)
Global	Current Rate of SLR [a]	NA	0.1044
Mississippi	Current RSLR in Mississippi [b]	NA	0.1357
GBNERR	Threshold Rate of SLR at GBNERR [c]	NA	0.2088
Contiguous US	Obs. Extrapolation	0.38	0.2204
Contiguous US	Low [d]	0.31	0.1798
Contiguous US	Intermediate-Low [d]	0.36	0.2088
Contiguous US	Intermediate [d]	0.4	0.232
Contiguous US	Intermediate-High [d]	0.46	0.2668
Contiguous US	High [d]	0.52	0.3016
Eastern Gulf	Obs. Extrapolation [d]	0.48	0.2784
Eastern Gulf	Low [d]	0.3	0.1740
Eastern Gulf	Intermediate-Low [d]	0.34	0.1972
Eastern Gulf	Intermediate [d]	0.38	0.2204
Eastern Gulf	Intermediate-High [d]	0.45	0.2610
Eastern Gulf	High [d]	0.51	0.2958

Table 2.5 *Amount added to tidal input to reflect SLR changes by 2100*

Source of values [a] = Wang et al., 2021, [b]= Wu et al., 2020, [c] = Sea Level Trends - NOAA Tides & Currents, [d]= Sweet et al., 2022.

Region	SLR Scenario	Amount with baseline of 2000 (m)	Adjusted to have a baseline of 2021 (m)
Global	Current Rate of SLR [a]	NA	0.284
Mississippi	Current RSLR in Mississippi [b]	NA	0.370
GBNERR	Threshold Rate of SLR at GBNERR [c]	NA	0.569
Contiguous US	Low [d]	0.6	0.474
Contiguous US	Intermediate-Low [d]	0.7	0.553
Contiguous US	Intermediate [d]	1.2	0.948
Contiguous US	Intermediate-High [d]	1.7	1.343
Contiguous US	High [d]	2.2	1.738
Contiguous US	Low [d]	0.6	0.474
Eastern Gulf	Intermediate-Low [d]	0.8	0.632
Eastern Gulf	Intermediate [d]	1.2	0.948
Eastern Gulf	Intermediate-High [d]	1.7	1.343
Eastern Gulf	High [d]	2.2	1.738

2.2.5 Statistical Analyses

Bayesian multi-level models were applied to determine the influence of salinity and elevation on DBH, height, and above- and belowground biomass during the first and second sampling events as well as the change in DBH and change in height which were averaged by subsite. Hierarchical Bayesian modeling decomposes complex relations into levels of data, process, and parameters (Clark, 2005; Hardy et al., 2021). Bayesian models generally use Markov Chain Monte Carlo simulations to derive the posterior distributions that make uncertainty readily quantifiable through the credible intervals (Wu et al., 2012; Hardy, 2018). I selected the best models for change in DBH and height based on deviance information criterion (DIC) and posterior predictive loss (PPL). The lower

the PPL or DIC, the better the model prediction (Hooten and Hobbs 2015). Transect and/or habitat served as grouping variables in the models. The different models had different combinations of elevation, salinity, and volume of trees as covariates. I normalized the covariates to speed up convergence and facilitate the comparisons of magnitudes of influence from these different covariates directly. Volume for the subsites was determined based on the 2020 average height (h) and DBH (2r) and considered the tree to be a cylinder calculating volume as $\pi r^2 h$. All models converged with 320,000 iterations based on the three chains I ran, and each chain was thinned every fourth iteration to reduce autocorrelation in the samples.

2.3 Results

2.3.1 Summary

The calibrated salinity simulation model determined that the maximum salinity of 29.72 ppt occurred at an elevation of 0.3 m NAVD 88, close to the mean high water level at GBNERR. By 2050 under the high RSLR scenario for the eastern gulf and the contiguous US, the maximum salinity moved up the elevational gradient by 0.40 m to 0.70 m NAVD88 with a maximum salinity of 30.91 and 35.06 ppt, respectively. By 2100, the maximum salinity and maximum salinity band moved beyond the observed elevation of 1.55 m NAVD88 for the intermediate-high and high RSLR scenarios for the eastern gulf and the contiguous US.

Based on the multi-level Bayesian models, during the first sampling event salinity was found to have a significantly negative impact on DBH and height. DBH was found to have a significantly negative relation to elevation during the second sampling event (2021). Both above- and belowground biomass of salt marsh and understory vegetation

were found to be significantly negatively related to elevation while positively related to salinity for both sampling events. When studying change in height, there was a significantly negative relation between salinity and the change in height of the ecotone on Transect 1 (prescribed fire in 2018). Additionally, the Transect 1's ecotone was significantly more negatively related to salinity than the Transect 1's forest and Transect 2's (control) ecotone. Finally, change in DBH did not have a significant relation with elevation, but was weakly positively related to volume while change in height was weakly negatively related to volume. I found there was a trade-off between growth in DBH and height as trees grew larger.

2.3.2 Salinity Model

After 96 trials, the model that produced the best results is shown in Figure 2.5. It predicted the highest porewater salinity of 29.72 ppt at an elevation of 0.3 m NAVD88. From the collected data, the highest average porewater salinity was also at this elevation. After this, the porewater salinity began to decrease before plateauing out at 7.51 ppt at an elevation of 0.5 m. This plateau represents the area outside of the influence of tidal inundation meaning it would be considered upland areas and outside the purview of this marsh model. The elevations where this plateau begins are indicated in figures with an *. At the marked elevation and above, soil porewater salinities should be disregarded because they cannot be accurately described by the marsh model.

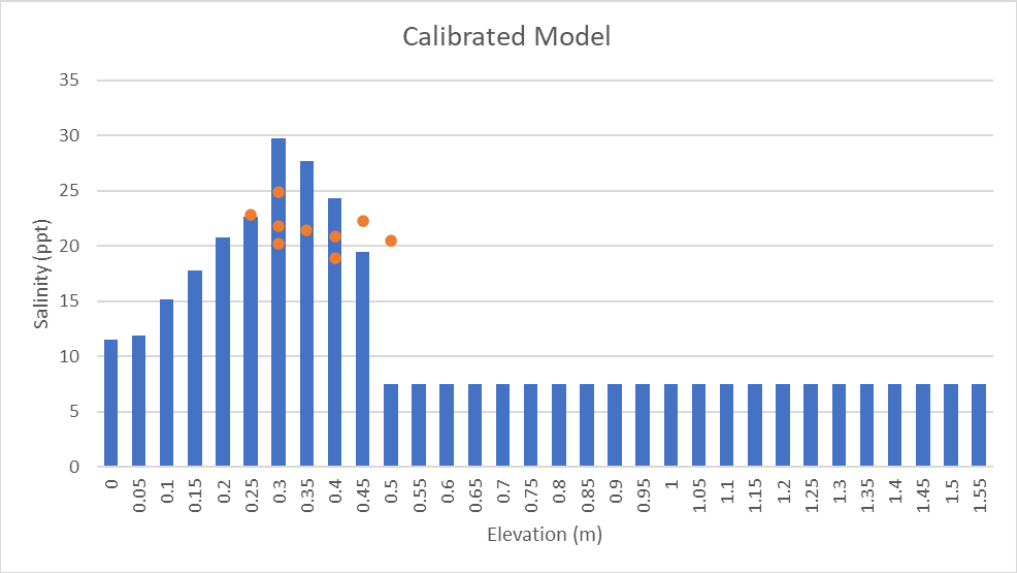

Figure 2.5 *Calibrated salinity model*

The blue bars represent the predicted salinity for each elevation interval. Orange points represent the collected salinity samples from 2021 to which the model was calibrated. * Indicates the beginning of elevations outside the purview of the model. At the indicated elevation and above, soil porewater salinities should be disregarded as the model cannot accurately simulate salinities outside of the marsh area. I kept the elevation up to 1.55 m to show patterns under different SLR scenarios.

The SLR scenarios by 2050 all moved the maximum salinity band up elevational gradient. The high scenarios for both the contiguous US and the eastern gulf moved the maximum salinity band up to 0.75 m NAVD88 (Figures 2.6 and 2.7). The observation-based extrapolation, low, intermediate-low, intermediate, and intermediate- high scenarios for the eastern gulf moved the salinity band up by 0.25, 0.15, 0.2, 0.2, and 0.25 m along the elevational gradient, respectively and for the contiguous US 0.2, 0.15, 0.2, 0.25 and 0.25 m, respectively from 0.45 m NAVD88. Both the threshold scenario for GBNERR and the intermediate-low scenario for the contiguous added the same amount to SLR by 2050 and both produced the largest increase in the maximum salinity with 35.60 ppt at an elevation of 0.6 m (Figures 2.6 and 2.7). By 2050 the global rate of SLR

moved the salinity band by 0.1 m while the RSLR in MS moved the band by 0.15 m from the calibrated model of 0.45 m NAVD88, where the maximum salinity band ended.

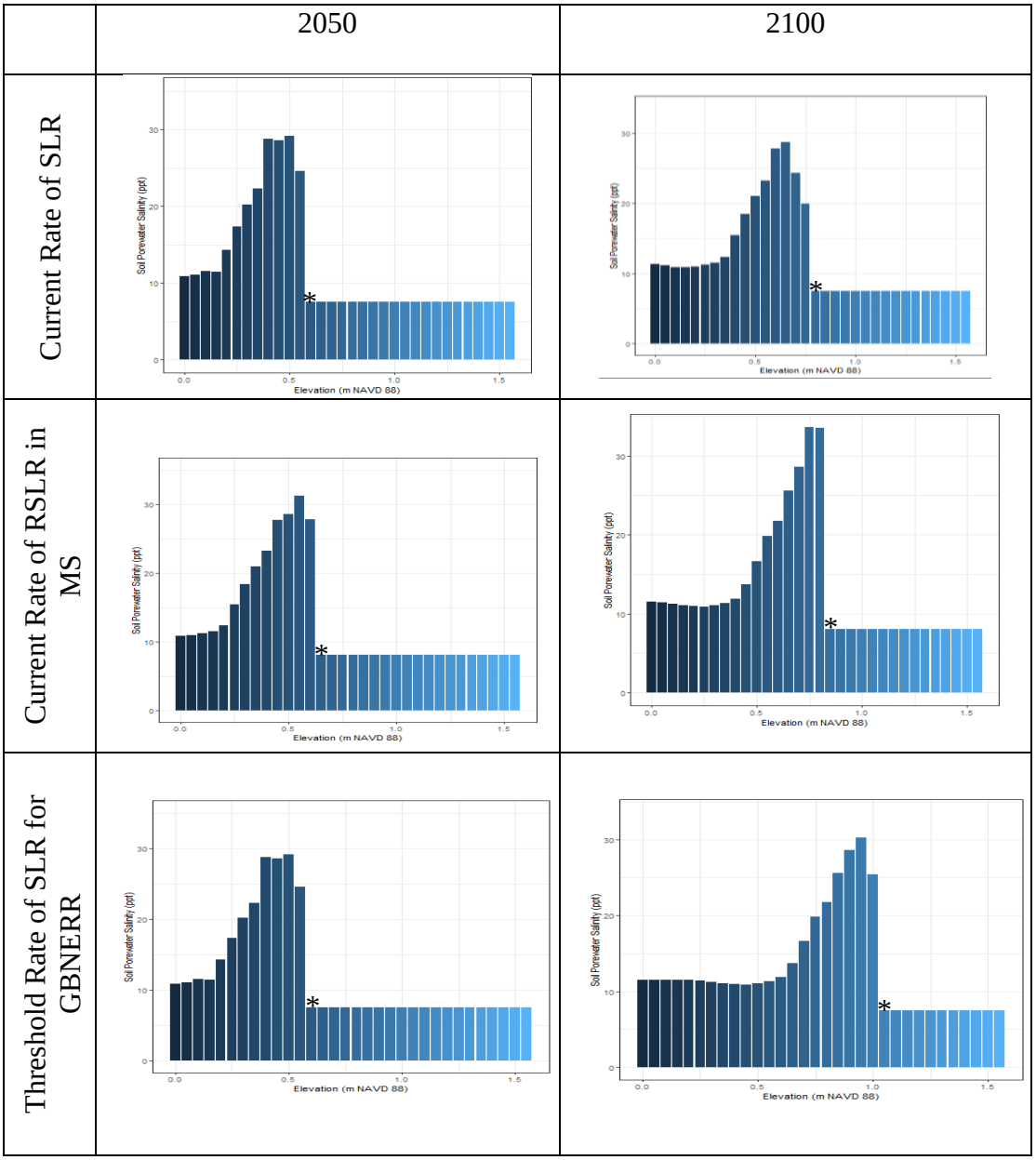

Figure 2.6 *Predicted salinities by elevation under the scenarios for the current global rate of SLR, the RSLR for MS, and the threshold rate of SLR for GBNERR by 2050 and 2100*

* Indicates the beginning of elevations outside the purview of the model. At the indicated elevation and above, soil porewater salinities should be disregarded as the model cannot accurately simulate salinities outside of the marsh area.

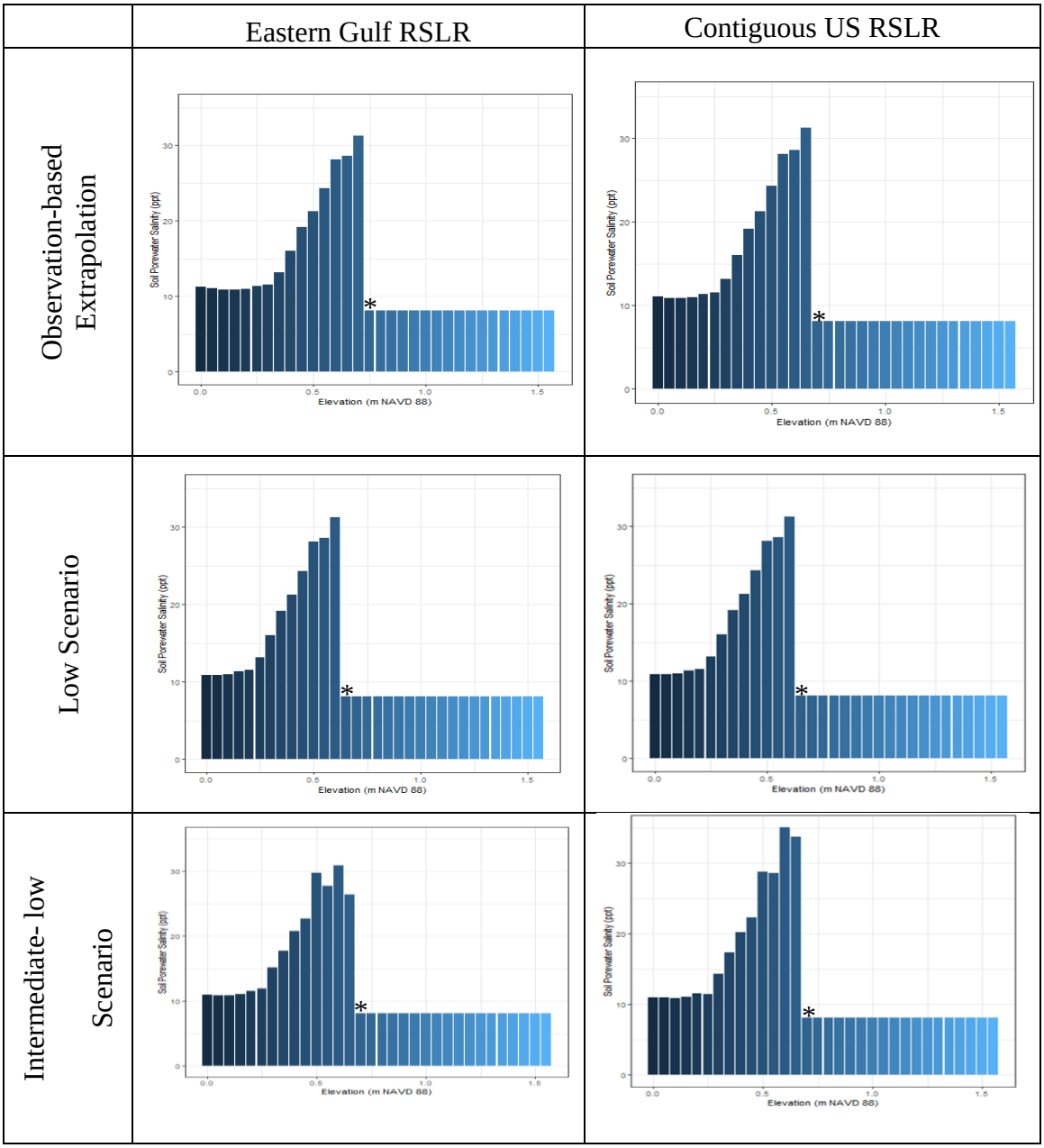

Figure 2.7 *Predicted salinities by elevation under observation-based extrapolation, low, intermediate-low, intermediate, intermediate-high, and high scenarios of RSLR for the eastern gulf and contiguous US by 2050*

* Indicates the beginning of elevations outside the purview of the model. At the indicated elevation and above, soil porewater salinities should be disregarded as the model cannot accurately simulate salinities outside of the marsh area.

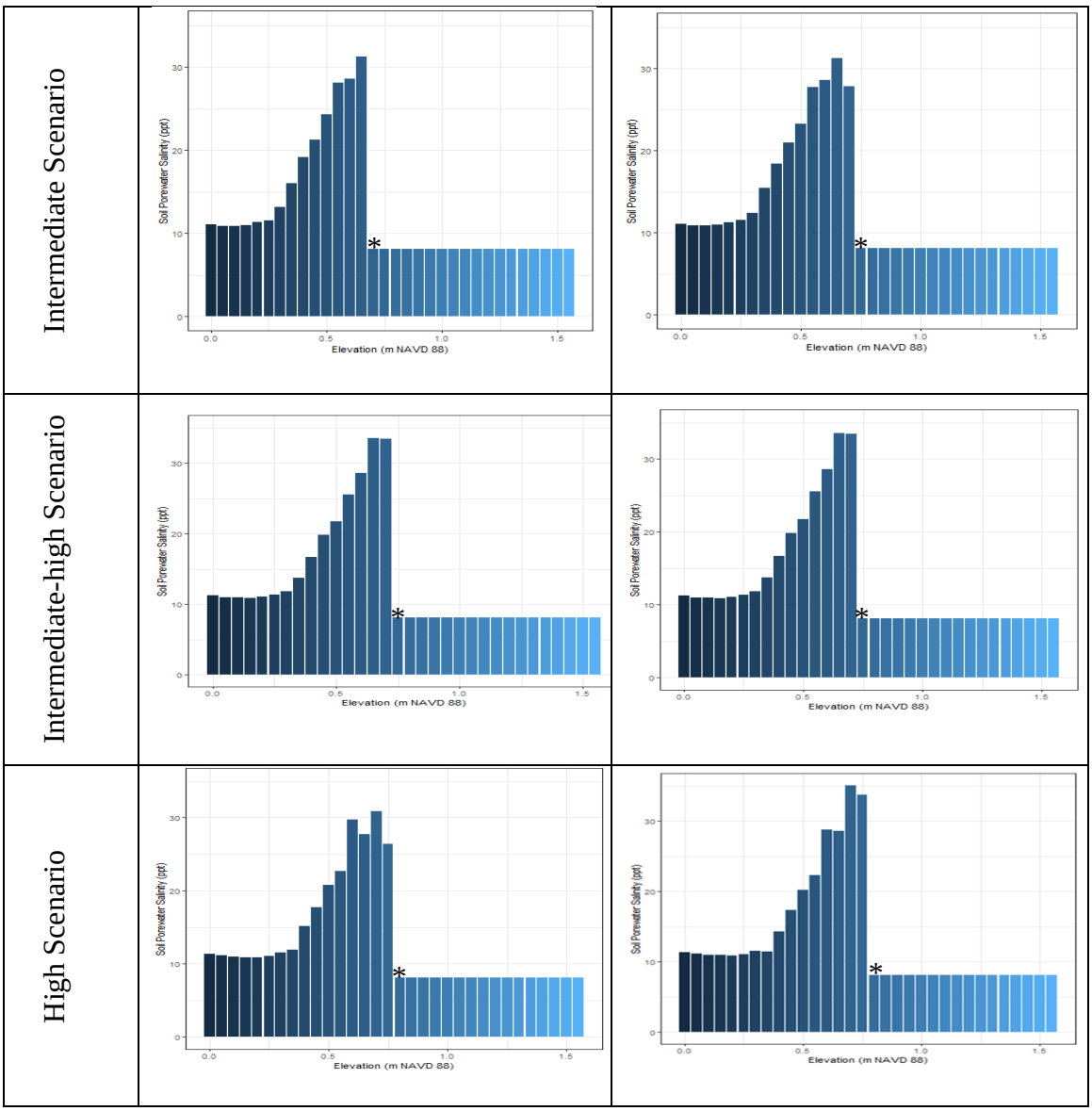

Figure 2.7 (continued)

Due to uncertainty, the reported SLR predictions for the low, intermediate, intermediate-high, and high scenarios for 2100 in the USGS Sweet et al. (2022) report were the same for the eastern gulf and the contiguous US, so the model produced the same results (Figure 2.8). The only difference between the two regions were for the intermediate-low scenario with 0.553 and 0.632 m being added to the tidal input for the

contiguous US and the eastern gulf, respectively. By 2100, the intermediate-high and high scenarios for the contiguous US and the eastern gulf were above the threshold for GBNERR. The low scenarios produced the largest maximum salinity on the observed elevation, increasing the maximum from 29.72 ppt at 0.3 m NAVD88 elevation for the calibrated model to 31.23 ppt at 0.9 m NAVD88. However, the intermediate-high and high scenarios pushed the maximum salinity band beyond that of the observed elevation range (Figure 2.8). It is likely that the high scenario would have produced the greatest increase in salinity had the observed range been greater. The salinity of 12.0 ppt from elevation of 0.0 to 1.5 m in those scenarios matches the initial salinity used in the model (Table 2.3). I did not consider possible salinity increase in the tidal water due to SLR.

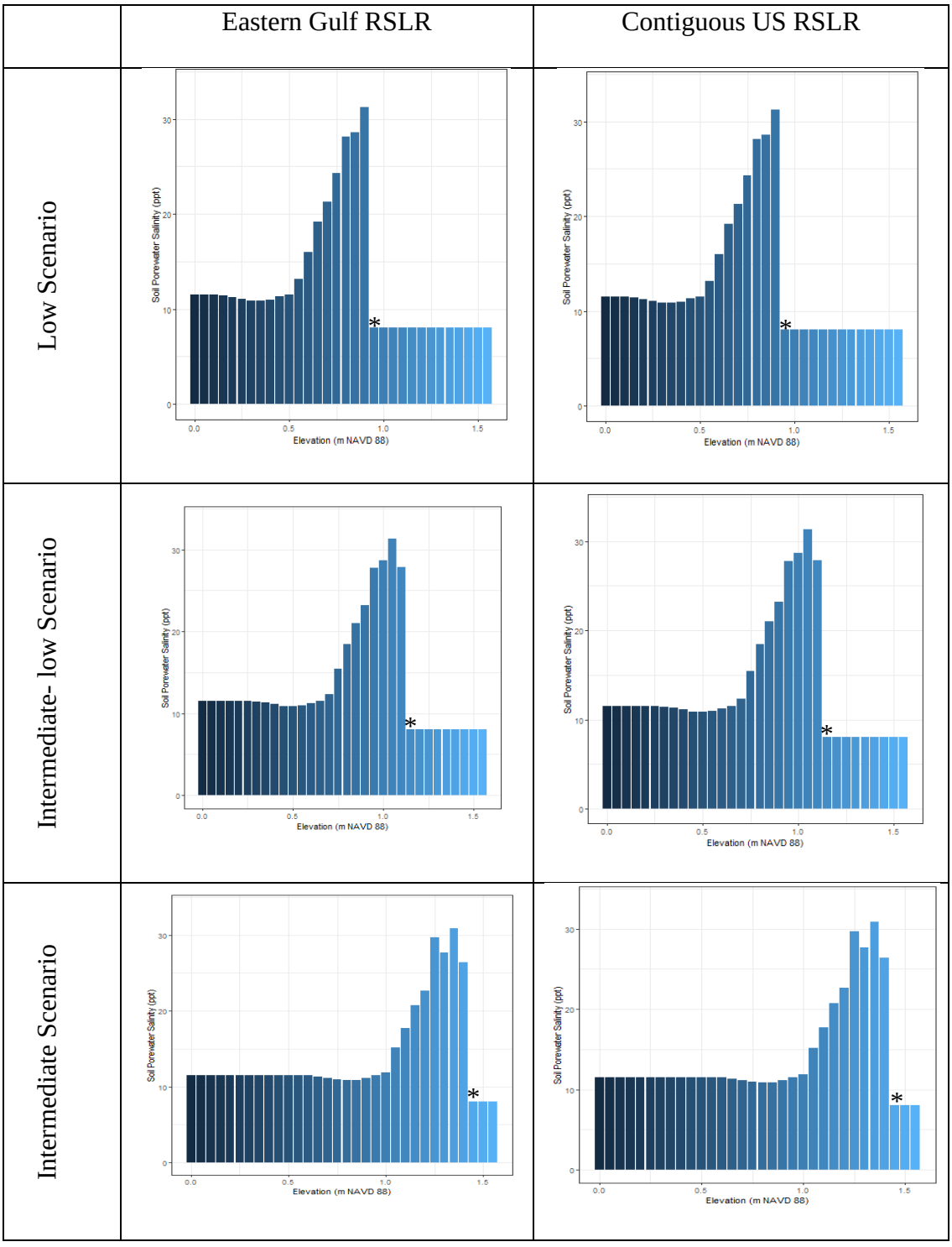

Figure 2.8 *Predicted salinities by elevation under low, intermediate-low, intermediate, intermediate-high, and high scenarios of RSLR for the eastern gulf and contiguous US by 2100*

* Indicates the beginning of elevations outside the purview of the model. At the indicated elevation and above, soil porewater salinities should be disregarded as the model cannot accurately simulate salinities outside of the marsh area.

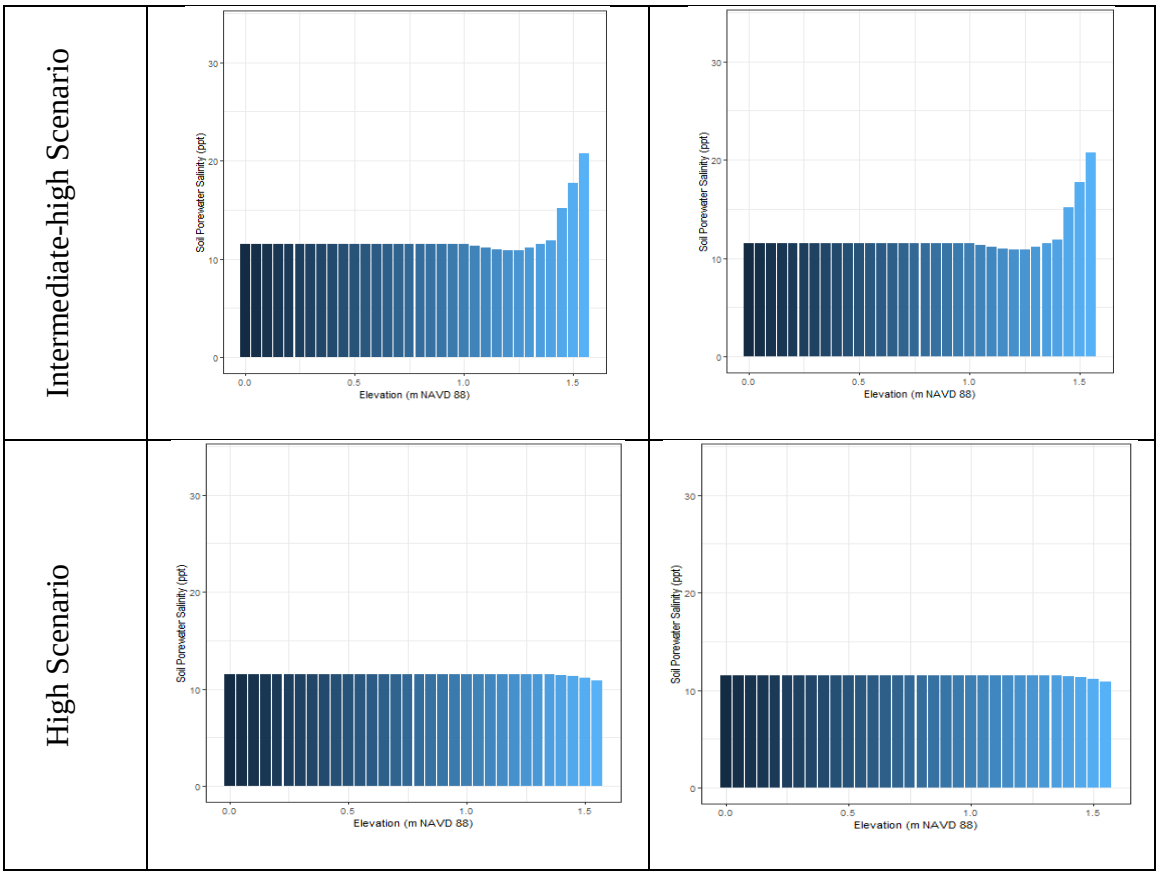

Figure 2.8 (continued)

2.3.3 Bayesian Models for Above- and Belowground Biomass and DBH and Height

During the first sampling event of the forest, DBH and height measurements were collected for 11 trees along Transect 1 and 142 trees along Transect 2. During the second sampling event the same trees were measured, and an additional 3 trees were measured along Transect 2 and 13 along Transect 3. Trees that had a DBH of less than 5 cm could only be found along Transect 2 (Figure 2.9 and 2.10). After running the Bayesian multi-level models looking at individual trees, DBH and height were found to be significantly negatively related to salinity during the first sampling event (Figure 2.11 and Figure 2.12). Transect 1 and Transect 3 were significantly larger than Transect 2 for both DBH and height if elevation or salinity's impact was not considered (Figures 2.11 and 2.12).

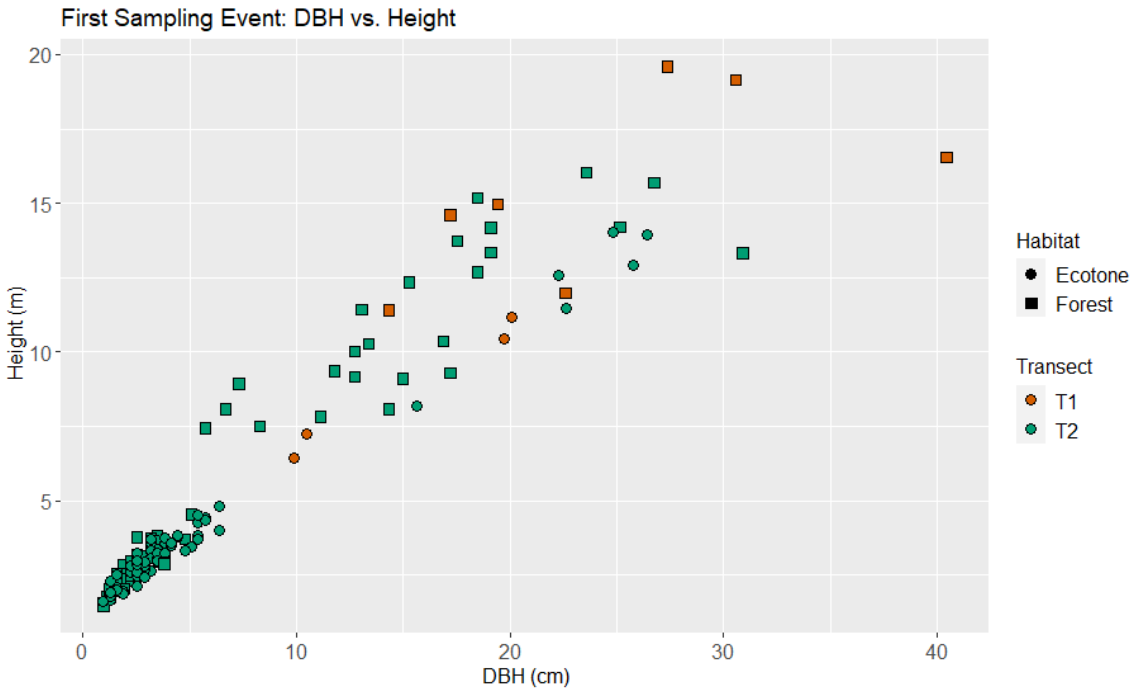

Figure 2.9 *Scatterplot depicting the height and DBH from the first sampling event*

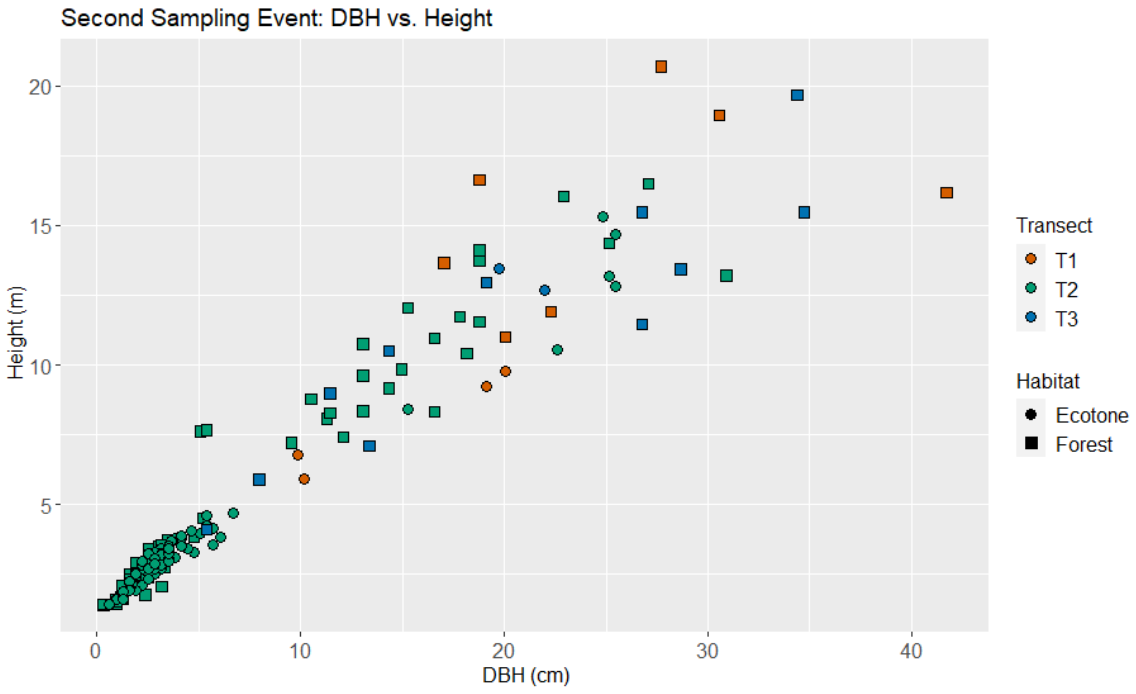

Figure 2.10 *Scatterplot depicting the height and DBH from the second sampling event*

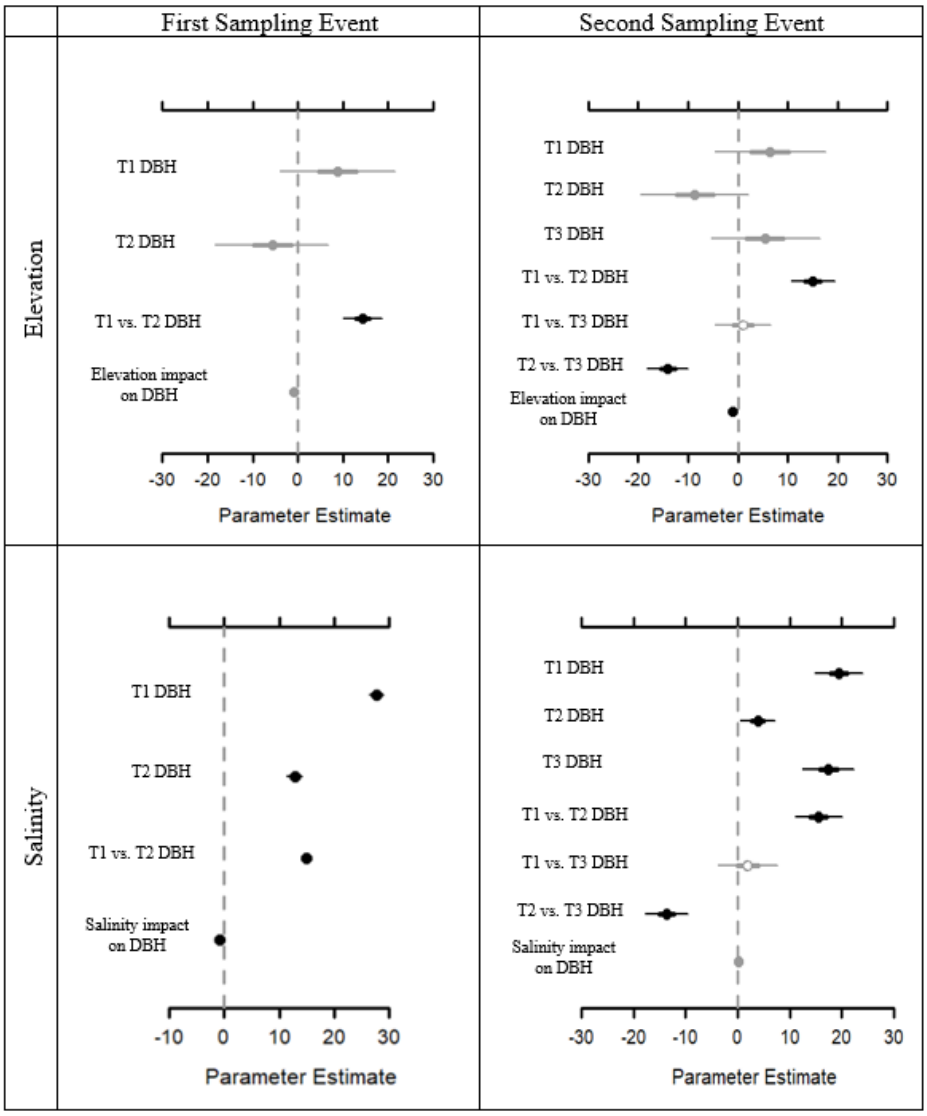

Figure 2.11 *Results of the Bayesian models showing the medians and credible intervals of the posterior distributions of the parameters depicting the impacts of elevation and salinity on DBH for the first and second sampling events*

T1 = Transect 1, T2 = Transect 2, and T3 = Transect 3. Lines extending from the circles represent the 95% credible interval. The thin line shows the 95% credible interval, and the thick line shows the 50% credible interval. The grey line with an open dot indicates that both 50% and 95% credible intervals contain 0, the grey line with a solid grey dot indicates that 50% credible interval does not contain 0 while 95% credible interval does, and the dark line with a solid dark dot indicates that 95% and 50% credible intervals do not contain 0. Plot generated using MCMCvis package in R (Youngflesh, 2018).

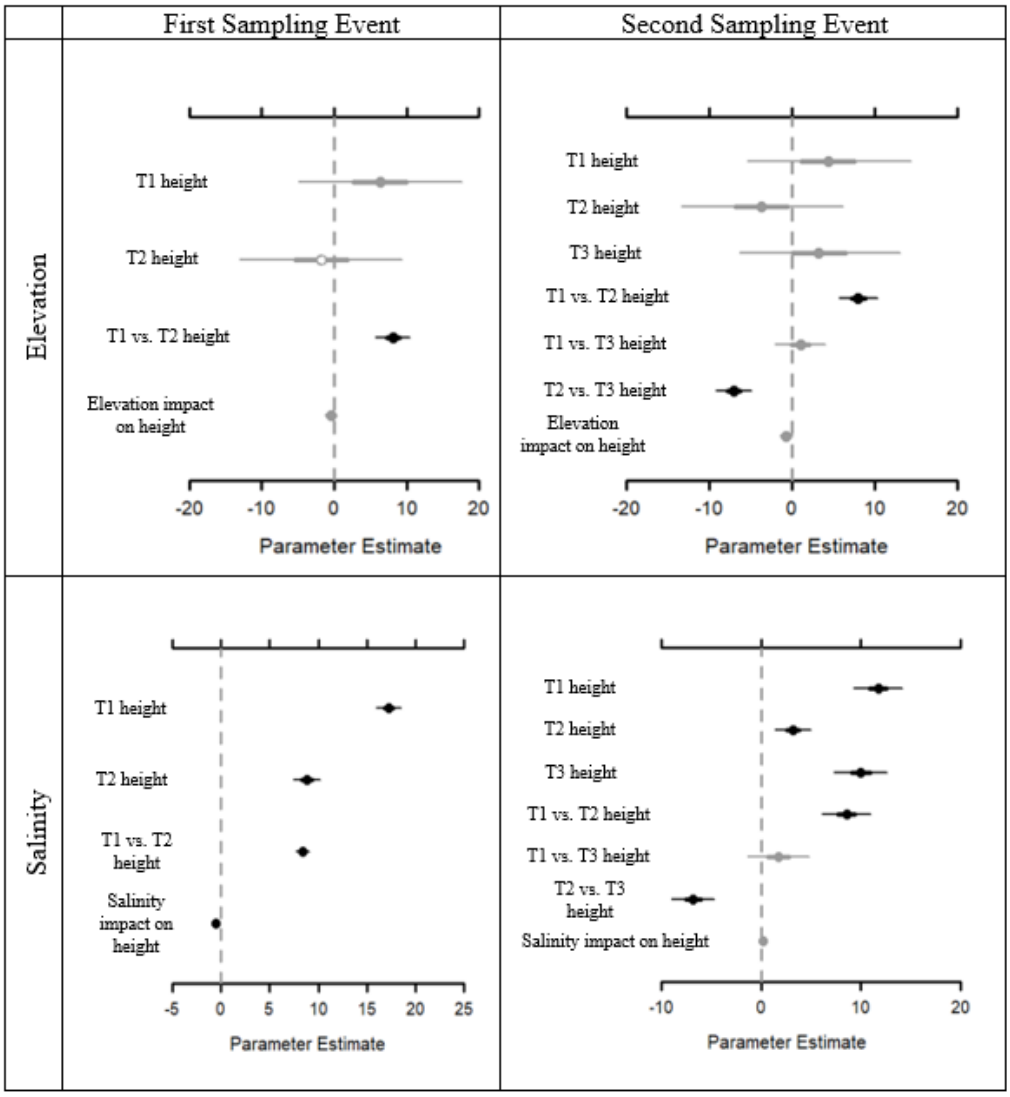

Figure 2.12 *Results of the Bayesian models showing the medians and credible intervals of the posterior distributions of the parameters depicting the impacts of elevation and salinity on height for the first and second sampling events*

T1 = Transect 1, T2 = Transect 2, and T3 = Transect 3. Lines extending from the circles represent the 95% credible interval. The thin line shows the 95% credible interval, and the thick line shows the 50% credible interval. The grey line with an open dot indicates that both 50% and 95% credible intervals contain 0, the grey line with a solid grey dot indicates that 50% credible interval does not contain 0 while 95% credible interval does, and the dark line with a solid dark dot indicates that 95% and 50% credible intervals do not contain 0. Plot generated using MCMCvis package in R (Youngflesh, 2018).

During 2020, above- and belowground biomass, and therefore soil porewater salinity, collection occurred for all subsites along Transect 1 and all subsites in the ecotone for Transect 2. During the 2021 field season above- and belowground biomass collection occurred at all subsites from Transects 1, 2, and 3 (Figures 2.13 and 2.14). Of the 30 subsites where collection occurred in both 2020 and 2021, the majority had an increase in aboveground biomass (n=24) with an average increase of 173.8, 334.2 and 944.0 g/m^2 for the forest, marsh, and ecotone, respectively. Soil porewater analysis was determined from the 2020 and 2021 field collection (Figures 2.15 and 2.16). Based on the ecotone in 2020, Transect 1 had a greater soil porewater salinity than Transect 2. In 2021, Transect 3 had the highest porewater salinity for the marsh and ecotone followed by Transects 2 and 1, respectively. Transect 2 had the highest porewater salinity in the forest followed by Transects 3 and 1, respectively. Marsh area had the highest salinities, in both years and for all transects. Soil porewater salinity was much higher during 2020 than 2021 with the porewater salinity of the forest in 2020 being comparable to that of the marsh porewater salinities in 2021 (Figures 2.15 and 2.16). The Bayesian multi-level models showed that there was a significantly negative relation between aboveground and belowground biomass and elevation for the for the first and second sampling events and a significantly positive relation between aboveground and belowground biomass and porewater salinity (Figures 2.17 and 2.18). Transect 1 had the greatest amount of aboveground biomass during the first and second sampling event. During the second sampling event, Transect 3 had the least amount of aboveground biomass (Figure 2.17). Transect 2 had the greater belowground biomass than Transect 1 during the first sampling

event, while Transect 3 had the greatest amount of belowground biomass during the second sampling event followed by Transect 1 and 2, respectively (Figure 2.18).

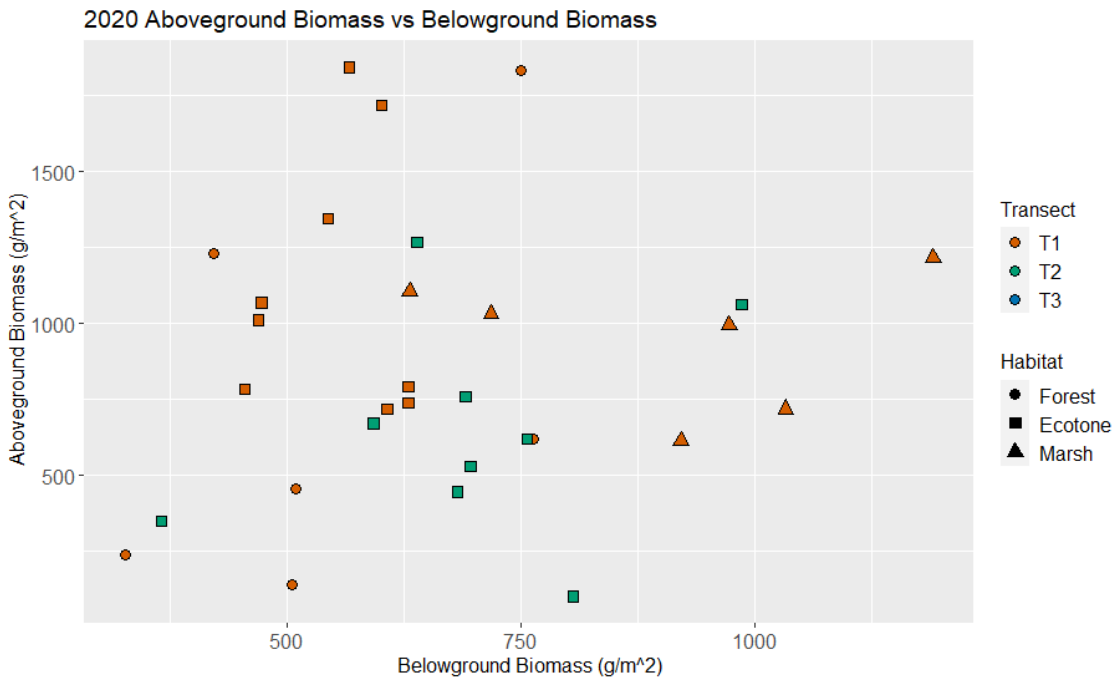

Figure 2.13 *Scatterplot showing above- and belowground biomass collected during the 2020 field season*

Note that Transect 3 was not sampled at this time nor was the forest or marsh for Transect 2.

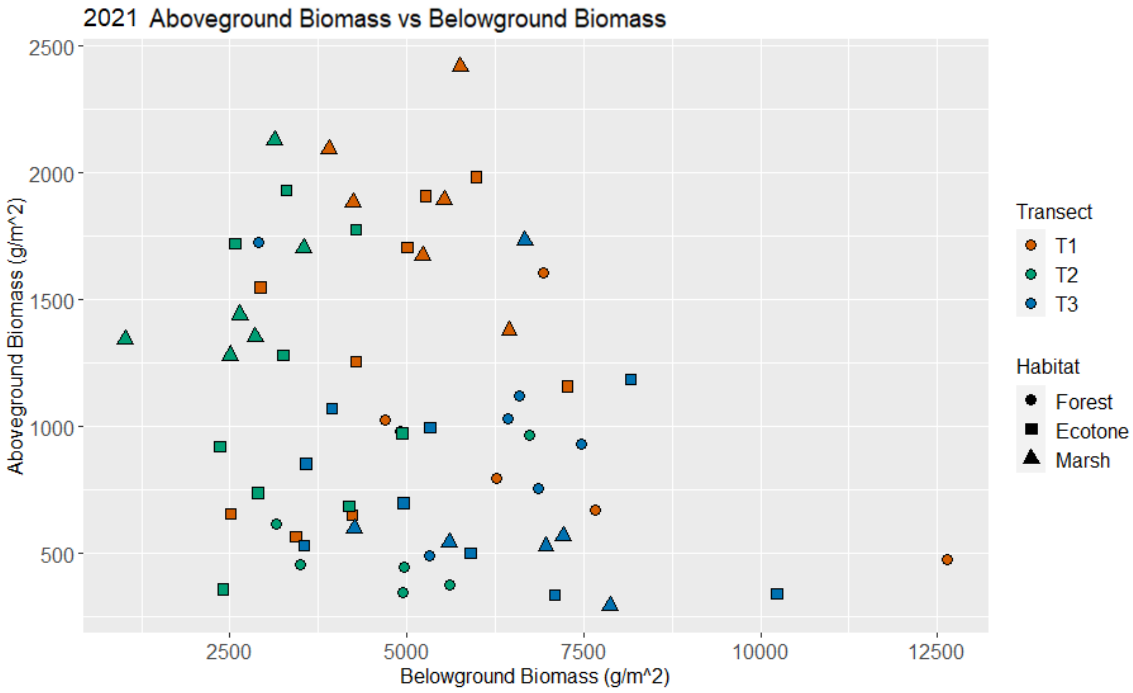

Figure 2.14 *Scatterplot showing above- and belowground biomass collected during the 2021 field season*

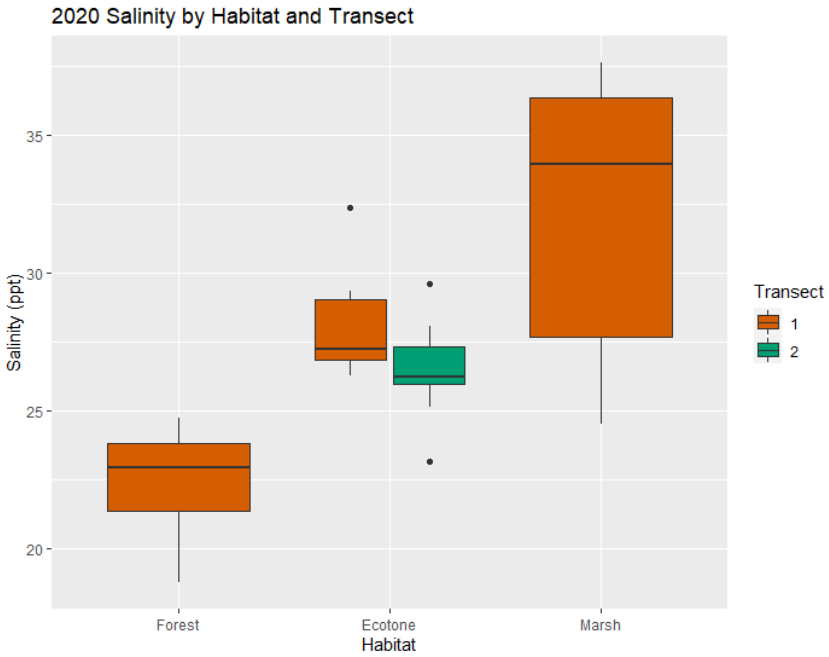

Figure 2.15 *Boxplot showing the 2020 soil porewater salinity by habitat and transect*

Note there was no soil porewater salinity measurements in the forest and saltmarsh of Transect 2 in 2020.

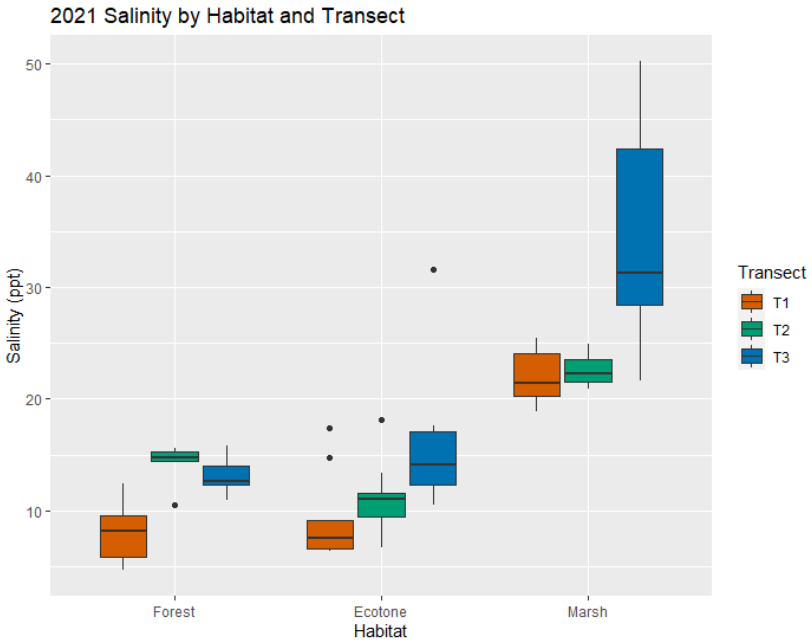

Figure 2.16 *Boxplot showing the 2021 soil porewater salinity by habitat and transect*

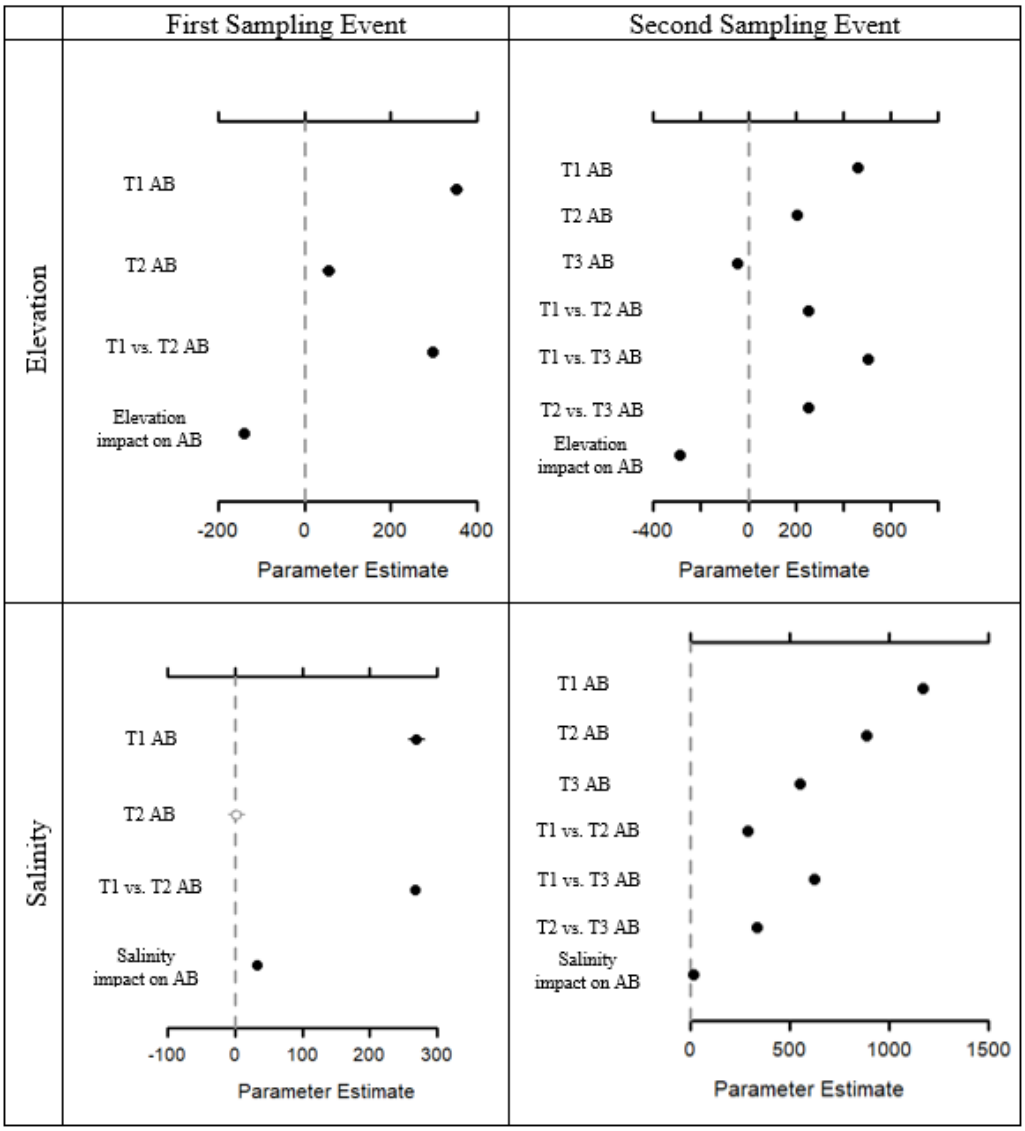

Figure 2.17 *Results of the Bayesian models showing the medians and credible intervals of the posterior distributions of the parameters depicting at the impacts of elevation and salinity on aboveground biomass for the first and second sampling events*

T1 = Transect 1, T2 = Transect 2, T3 = Transect 3, and AB = aboveground biomass. The thin line shows the 95% credible interval, and the thick line shows the 50% credible interval. The grey line with an open dot indicates that both 50% and 95% credible intervals contain 0, the grey line with a solid grey dot indicates that 50% credible interval does not contain 0 while 95% credible interval does, and the dark line with a solid dark dot indicates that 95% and 50% credible intervals do not contain 0. Plot generated using MCMCvis package in R (Youngflesh, 2018).

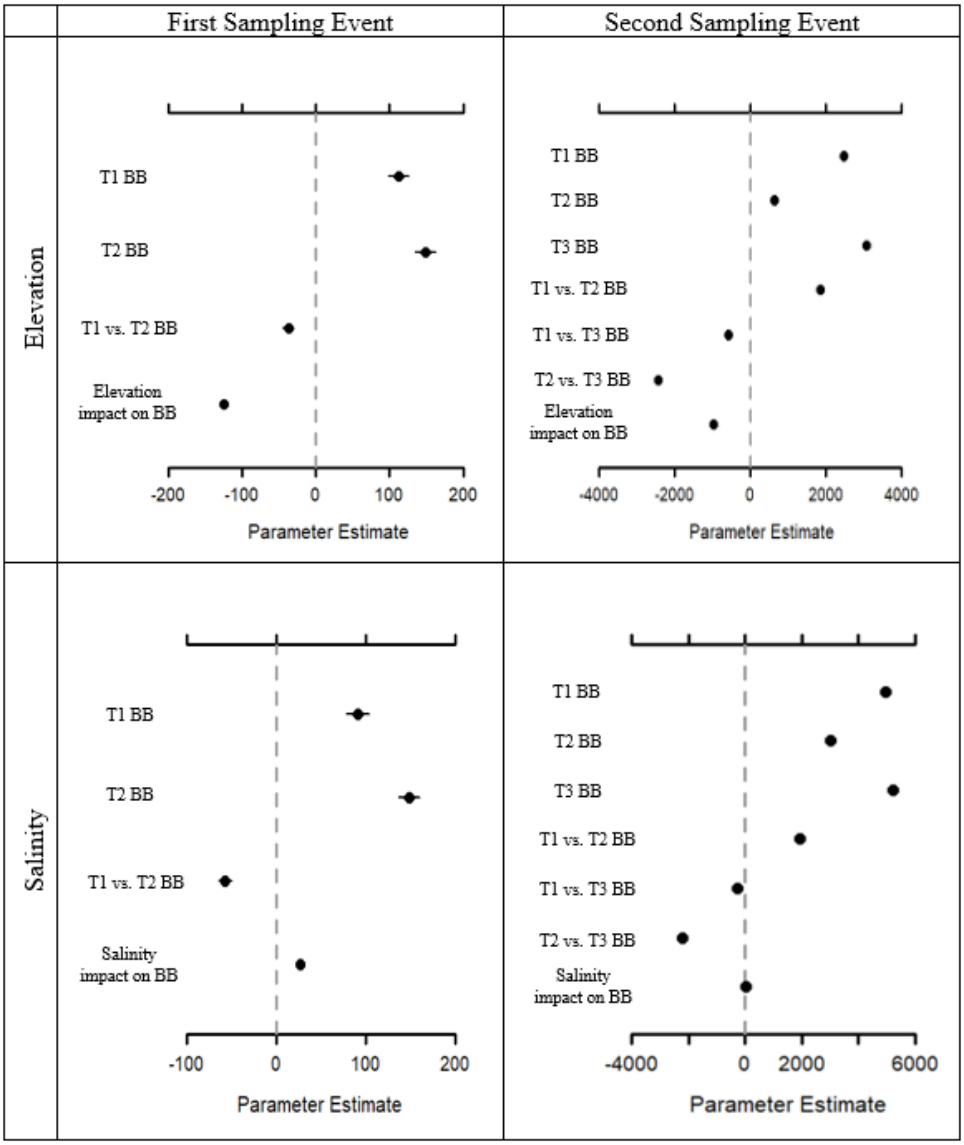

Figure 2.18 *Results of the Bayesian models showing the medians and credible intervals of the posterior distributions of the parameters depicting at the impacts of elevation and salinity on belowground biomass for the first and second sampling events*

T1 = Transect 1, T2 = Transect 2, T3 = Transect 3, and BB = belowground biomass. The thin line shows the 95% credible interval, and the thick line shows the 50% credible interval. The grey line with an open dot indicates that both 50% and 95% credible intervals contain 0, the grey line with a solid grey dot indicates that 50% credible interval does not contain 0 while 95% credible interval does, and the dark line with a solid dark dot indicates that 95% and 50% credible intervals do not contain 0. Plot generated using MCMCvis package in R (Youngflesh, 2018).

2.3.4 Bayesian Models for Change in Height

Ten models of tree height change were developed and compared. In these ten models, I considered different combinations of covariates of elevation, soil porewater salinity, and tree volume and whether their effect on tree height change varied by transect and/or habitat. The best model, based on the lowest DIC and PPL, was model number 6 (Table 2.6). The model converged well as all parameters had an upper credible interval that was less than 1.1 (Table 2.7). Model 6 did not consider elevation in influencing change in height but did consider salinity. The best prediction was estimated when salinity's impact varied by transect and habitat.

Table 2.6 *DIC and PPL values for models tested*

X represents parameters that varied by transect, O represents parameters that varied by habitat. A blacked-out box means that the parameter was not included in the model. Best model is bolded.

Model	a (intercept)	b (salinity)	c (elevation)	d (volume)	DIC	PPL
1		XO			20.5	3.195379
2				XO	27.58	4.561839
3		X		X	34.71	6.642683
4		X			32.26	5.961515
5				X	32.93	6.147328
6		**XO**			**20.34**	**3.173771**
7				XO	27.48	4.551061
8		X		X	34.84	6.705757
9		X			32.36	6.004599

Table 2.7 *Upper credible intervals for parameters used*

Parameter (description)	Point est.	Upper C.I.
a (intercept)	1	1
b[1,1] (salinity for transect 1 ecotone)	1	1
b[2,1] (salinity for transect 1 forest)	1	1
b[1,2] (salinity for transect 2 ecotone)	1	1
b[2,2] (salinity for transect 2 forest)	1	1
d (volume)	1	1

The model shows that there was a significantly negative effect of salinity on change in height for the ecotone on Transect 1, with a mean of -0.28 for the coefficient of salinity and the 95% credible interval being less than 0 (Figure 2.19). Volume was also negatively related to change in height. However, this is a weaker relation with a mean of -0.21 for its coefficient and only the 50% credible interval being less than 0. Intercept, salinity at Transect 1 forest, salinity at Transect 2 ecotone and forest showed no significant relation with change in height.

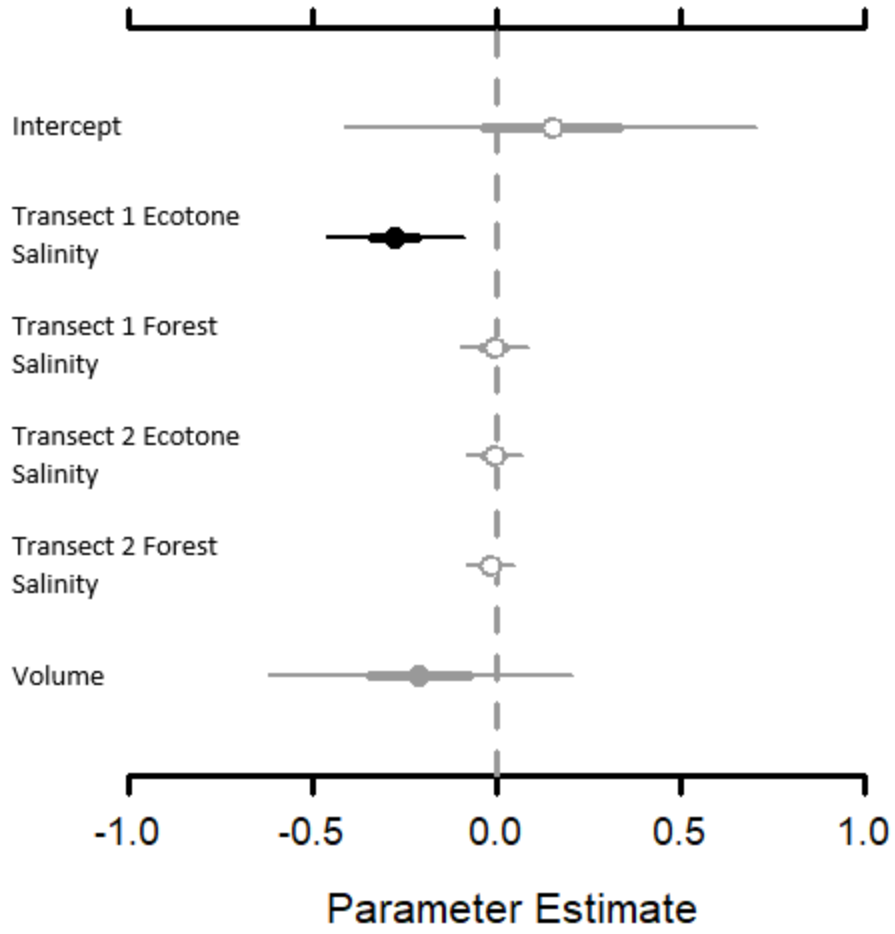

Figure 2.19 *Medians and credible intervals of the posterior distributions of the parameters depicting the relation of salinity and volume on change in height with salinity varying by transect and habitat*

The thin line shows the 95% credible interval, and the thick line shows the 50% credible interval. The grey line with an open dot indicates that both 50% and 95% credible intervals contain 0, the grey line with a solid grey dot indicates that 50% credible interval does not contain 0 while 95% credible interval does, and the dark line with a solid dark dot indicates that 95% and 50% credible intervals do not contain 0. Plot generated using MCMCvis package in R (Youngflesh, 2018).

When comparing the effect of salinity between transect and habitat type, Transect 1 ecotone change in height was significantly more negatively related to salinity than the forest. Transect 1 ecotone was also significantly more negatively related to salinity than Transect 2 ecotone (Figure 2.20). Difference of parameters had the 95% credible interval

less than 0. There was no significant difference of the salinity's impact on height change between the forest and ecotone on Transect 2 or between the forest of Transect 1 and 2.

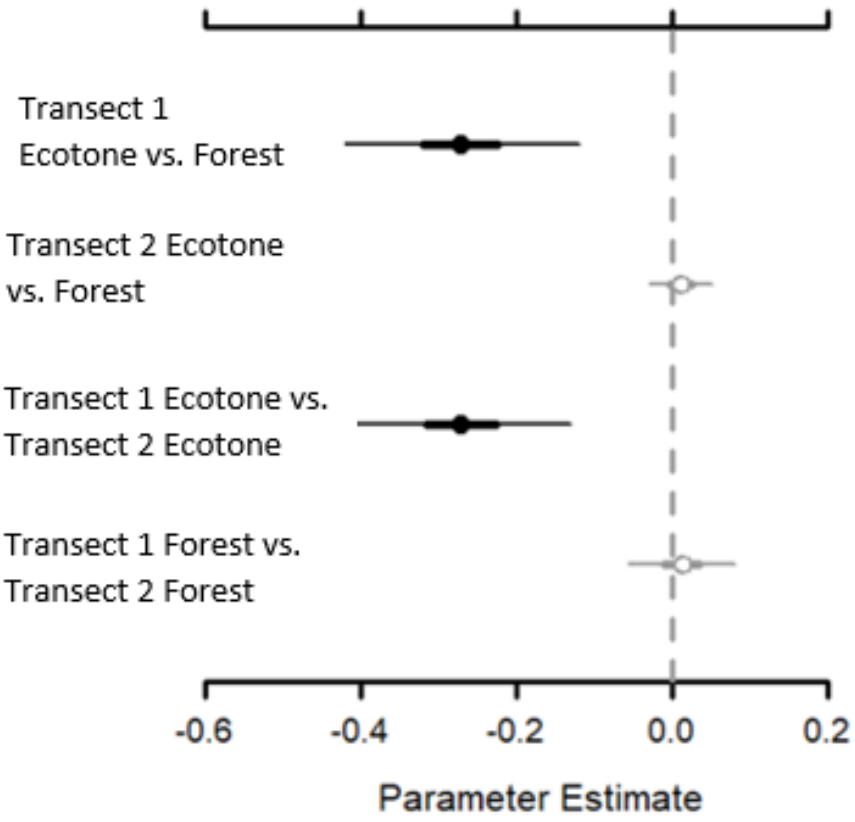

Figure 2.20 *Median and credible intervals of the posterior distributions of the parameters showing the difference of salinity's effect on change in height by habitat and transect*

The thin line shows the 95% credible interval, and the thick line shows the 50% credible interval. The grey line with an open dot indicates that both 50% and 95% credible intervals contain 0, the grey line with a solid grey dot indicates that 50% credible interval does not contain 0 while 95% credible interval does, and the dark line with a solid dark dot indicates that 95% and 50% credible intervals do not contain 0. Plot generated using MCMCvis package in R (Youngflesh, 2018).

2.3.5 Bayesian Models for Change in DBH

I compared four different models of change in DBH (Table 2.8), and found the best model had elevation and volume as the covariates and their impact on change in DBH did

not differ by transect. I did not consider salinity here as our preliminary model runs showed salinity did not impact DBH change. Based on the credible intervals of the parameters for elevation and volume (Figure 2.21), elevation did not have effect on DBH change while volume had some positive effect on DBH change. The larger the trees, the higher rate of DBH growth, opposite to the volume's impact on height change.

Table 2.8 *Models of DBH change (bolded is the best model)*

	Intercept	Elevation	Volume	DIC	PPL
Model 1	Vary by transect	Not vary by transect	Not included	128.4	1288.825
Model 2	Not vary by transect	Not vary by transect	Not included	128.4	1298.134
Model 3	Not vary by transect	Vary by transect	Not included	128.6	1280.337
Model 4	**Not vary by transect**	**Not vary by transect**	**Not vary by transect**	**126.8**	**1162.872**

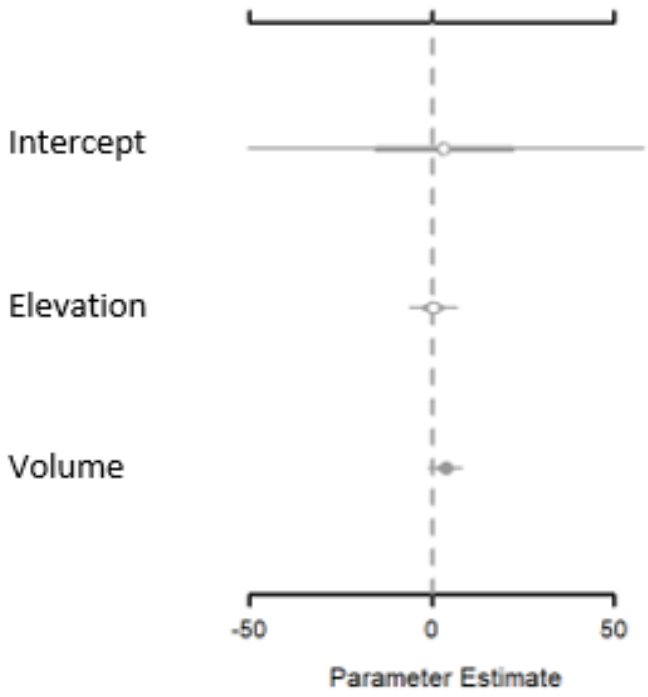

Figure 2.21 *Median and credible intervals of the posterior distributions of intercept, effect of elevation, and effect of volume on change of DBH*

The thin line shows the 95% credible interval, and the thick line shows the 50% credible interval. The grey line with an open dot indicates that both 50% and 95% credible intervals contain 0, the grey line with a solid grey dot indicates that 50% credible interval does not contain 0 while 95% credible interval does, and the dark line with a solid dark dot indicates that 95% and 50% credible intervals do not contain 0. Plot generated using MCMCvis package in R (Youngflesh, 2018).

2.4 Discussion

The SLR scenarios that were applied to the calibrated salinity model each drove the maximum salinity band up the elevation gradient. This supports Wang et al. (2007) findings that the mean higher high water level is the driving force behind the maximum salinity band. The high water level at GBNERR is 0.273 m NAVD88 and mean higher high water is 0.302 m NAVD88. This coincides with the maximum salinity of the calibrated model at 29.72 ppt at 0.3 m NAVD - supporting that idea that

evapotranspiration plays an important role in areas that have less frequent tidal inundation (Adam, 1990; Wang et al., 2007). Because tide is a driving force behind the maximum salinity band, and with each sea level rise scenario the maximum salinity band pushed further up the elevation gradient, this shows support for marsh migration landward as a response to SLR. The tide will create salinity stress at higher elevations as inundation occurs higher up the elevational gradient. It is important to note that the 2021 data with which the model was calibrated to was collected in August 2021. 2021 was an extremely wet year in Mississippi with June, July, and August each ranking in the top 10 wettest compared the same months in previous years since 1895. This is based on the Palmer Drought Severity Index (PDSI) which uses temperature and precipitation data to estimate relative dryness (NOAA National Centers for Environmental Information; Dai, 2019). August of 2021 was the wettest August on record in Mississippi with a PDSI of 5.76 (NOAA National Centers for Environmental Information). Furthermore, April and May both had a PDSI over 2.0 indicating an unusually moist period. This would have created a greater than normal input of freshwater to GBNERR which may have led to lower than normal soil porewater salinities. Finally, the elevation range observed (0-1.55 m) is not applicable to all areas. This range works well for GBNERR, but would have to be adjusted if the salinity model is calibrated to a different area.

The Bayesian regressions showed a significantly negative relationship between elevation and DBH during the second sampling event. This result is counter intuitive as it would be expected that larger trees would occupy higher elevations. However, I did not consider age of the trees. This finding is likely driven by the large number of young trees on Transect 2. Transect 1 and 3 consisted of fewer, but larger trees. During the first

sampling event there were significantly negative relationship with DBH and height to salinity, suggesting that larger trees are likely to be found in locations with less salinity stress. This finding is supported by that of Conner et al. (2022) which found there to be a negative relation between porewater salinity and woody growth of different tree species in tidal freshwater forested wetlands. Again, results for height and DBH are likely influenced by the large number of smaller trees that were found on Transect 2. Future analysis should look at trees that have a DBH < 5 cm and a DBH > 5 cm separately to make the transects more comparable. Also, analysis for the first sampling event for salinity could only be carried out for areas that had soil porewater salinity data (all of Transect 1 and ecotone of Transect 2).

When looking at above- and belowground biomass of understory vegetation, both were significantly negatively related to elevation while significantly positively related to salinity during the first and second sampling events. The results for belowground biomass having a positive relation to salinity is supported by Alldred et al. (2017). This study found that belowground biomass was enhanced up to 70% in high salinity marshes. Alldred et al. (2017) hypothesize that this is a result of plants allocating more growth to belowground biomass as a response to sulfide stress, in which more growth will help to aerate the sediment and facilitate sulfate oxidation. The positive relation between salinity and aboveground biomass, which includes the marsh as well as the understory vegetation of the ecotone and forest is counter intuitive. Generally, it is expected that aboveground biomass should increase as salinity stress decreases (Więski et al., 2010). However, the

aboveground biomass does not include the biomass of the trees. If the tree biomass was included in aboveground biomass estimation, there would likely be a different trend.

In order to infer the impact of fire on vegetation, I studied base DBH, height, and biomass that did not consider the impact of elevation or salinity. The findings that tree DBH and tree height at the fire impacted transect was larger than the DBH at the control transect nearby are mainly due to the absence of younger trees at the fire impacted transect. The absence of younger trees may be due to removal of seedlings/saplings during the prescribed fire event. Sharma et al. (2020) found that slash pines less than 3 m were unlikely to survive a prescribed fire event. However, prescribed fires are necessary to remove understory vegetation and to create favorable conditions for new recruitment and prevent slash pine stands converting to mixed-hardwoods (Monk, 1968). The lack of success of recruitment two to three years after the prescribed fire on Transect 1, may be explained by higher salinity in 2020 when hurricanes were active on the Mississippi Gulf Coast with forest salinities in 2020 being comparable to that of the marsh areas in an extremely wet year of 2021 (Figures 2.15 and 2.16). In terms of above- and belowground biomass of salt marsh and understory vegetation, I also found higher values at the fire impacted transect compared to the control transect nearby. This information, combined with lack of recruitment success at the fire impacted transect, suggests salt marsh vegetation is likely to grow more successfully after prescribed fire and therefore prescribed fire may facilitate landward migration of salt marshes.

The best Bayesian multi-level model for change in height included variation by transect and habitat for salinity's impact. The results showed that there was a significant negative relation between salinity and change in height for the ecotone habitat of

Transect 1. Again, Transect 1 represents an area where fire management occurs. When compared to Transect 2, Transect 1 had a significantly more negative relation between salinity and change in height for the ecotone with the 95% credible interval below zero. This significantly more negative relation may be related to impacts of fire management, again showing that fire may be able to facilitate marsh migration through removal of understory vegetation as well as altering the hydrological cycle (Glenn et al., 2013).

Finally, volume which impact did not differ by habitat or transect, was found to have a weakly negative relation with change in height (50% of the credible interval was below 0). The relation may be explained by change in allocation of mass as a tree matures. Where younger trees put more energy into growth in height, mature trees slow down growth in height, but put more energy into growth of diameter (supported by my model of DBH change) or leaf area (Stephenson et al., 2014).

While these models serve as great basis for understanding the impacts of salinity, there is a lot of uncertainty due to the sample size of the data set. This research could benefit from a larger sample size over a longer period of time. The calibrated salinity model could be more robust if it was calibrated to more data points at more varying elevations. The salinity model also has uncertainty built into it due to the model structure. This model is not spatial, so it does not consider the lateral flow of the water and horizontal movement of salt.

The next step is to integrate my salinity model predictions into the height change model to predict how sea-level rise can affect height change in the future. All the findings from my research will facilitate development of a mechanistic model to predict landward migration of salt marshes. Data from this chapter will be used to predict how the abiotic

factors such tidal inundation, climate, and evapotranspiration will drive soil porewater salinity up the elevational gradient as shown by the results of the simulation model for salinity. Additionally, this chapter will inform how the abiotic factor of soil porewater salinity will then influence the biotic factors such as above- and belowground biomass of understory vegetation as well as growth of uplands slash pines. In addition, historical land cover changes derived in Chapter 1 can help calibrate the mechanistic model.

2.5 Conclusion

The salinity model determined that as SLR increases, the maximum salinity band will move up the elevation gradient. This supports landward migration as salinity stress will continue to move up in elevation potentially freeing up space for marsh to migrate into. Using Bayesian multi-level models, I found DBH and height to be negatively related to salinity during the first sampling event. Above- and belowground biomass were significantly negatively related to elevation, but significantly positively related to salinity during the first and second sampling events. Finally, change in height was significantly negatively related to salinity for the ecotone on Transect 1, and Transect 1 change in height was significantly more negatively impacted by salinity than Transect 2. Based on this study, there is evidence that marsh could migrate landward at GBNERR and be facilitated by prescribed fire management.

CHAPTER III – CONCLUSIONS AND FURTURE DIRECTIONS

3.1 Conclusions

In my first chapter, I looked at the historical land cover changes over two-time intervals since 1955 at the Grand Bay National Estuarine Research Reserve which receives little sediment inputs and is a higher saline estuary and the Pascagoula River delta which receives large freshwater and allochthonous sediment inputs. The analysis showed that there is evidence of landward migration and the rate at which forest transitioned to marsh increased from the first-time interval to the second. However, these gains in marsh area are much less than the losses at the water's edge. The greatest percent of forest that transitioned to marsh was occurring at elevations between the current mean tidal level and mean high water level at both study sites. This finding is consistent with that of Wang et al., 2007. Wang et al. (2007) determined that there is a maximum salinity band which is driven by the mean higher high water level or mean high water level in a diurnal system. Increased salinity stress at the forest-marsh boundary likely caused a dieback of the glycophytic vegetation, freeing habitat for marshes to migrate into.

My second chapter used field data that was collected between 2020 and 2021 at the Grand Bay National Estuarine Research Reserve to look at soil porewater salinity impacts. I calibrated a soil porewater salinity simulation model from Wang et al. (2007) to predict soil porewater salinity every 0.05 m over an elevational gradient from 0 to 1.55 m. The model was then adjusted to mimic the different sea level rise scenarios described in Sweet et al. (2022). Once calibrated, the model showed that the maximum soil porewater salinity occurred at 0.3 m. Under different SLR scenarios, the maximum salinity and the maximum salinity band was pushed up the elevational gradient. This

supports the potential for landward migration of marshes as the salinity stress will increase further up in elevation as SLR occurs.

Using Bayesian multi-level modeling, I found that diameter at breast height and height of slash pines were negatively related to salinity during the first sampling event. This result shows that larger trees were likely to be found in areas with less salinity stress. Furthermore, I found that salinity was positively related to the belowground and aboveground biomass of the marsh and understudy vegetation for all transects. The results for belowground biomass are supported by Alldred et al. (2017) whose research found that belowground biomass was enhanced up to 70% in high salinity marshes. The positive relation for salinity and aboveground biomass is not supported (Wieski et al., 2010), but this is likely due to aboveground biomass including marsh vegetation as well ecotone and forest understory vegetation but not the biomass of the trees. Change in height was significantly negatively related to salinity in the ecotone of the transect with fire management and this relation was more significantly negative than that of the ecotone of the transect in a non-managed area. This, combined with higher above and belowground biomass at Transect 1 (with prescribed fire) compared to Transect 2 (no fire impact), gives evidence that fire management may help to facilitate the migration of coastal marshes, as trees in this area are more negatively impacted by higher salinities.

This research provided valuable information and insights into the historical land cover change of two southeastern estuaries along the Mississippi coast as well as impacts of soil porewater salinities in the forest, marsh, and ecotone habitats and the potential for landward migration of marshes. However, this research serves as a basis, a larger sample size would need to be collected to make these analyses more robust. This study would

benefit from multiple more transects being setup along the control areas that are not fire managed, as well as in different areas within the Grand Bay National Estuarine Research Reserve boundary. Finally, measurements of height and diameter at breast height need to be taken over a longer timescale to get more accurate depictions of changes over time.

3.2 Future Directions

To further this work, results from this research will be used to facilitate the development of a mechanistic model to predict landward migration of salt marshes. The core of this model will look at inter- and intraspecific competition of four functional groups: mature trees, saplings, understory vegetation, and salt marsh vegetation and how the biotic factors interact with abiotic factors such as soil porewater salinity, climate, and fire management (Figure 1.3). Chapter 1 results will serve to calibrate to the model through the historical land cover change. The work done in chapter two will inform how soil porewater salinity will influence the biotic factors of the understory and marsh vegetation as well as the trees. Above- and belowground biomass can serve as a proxy for primary production of the marshes and understory vegetation. Data on tree height and DBH, through allometric equations, can be used to determine tree biomass and serve as a proxy for primary production of the forest. Additionally, by comparing the fire managed vs non-fire managed transects I can inform how fire will impact biotic factors. More work will need to be done to understand competition based on light, intraspecific competition between mature and sapling trees, as well impacts of evapotranspiration. This information will be found by looking into more literature or running additional analyses on the data I collected. In addition to the field data described throughout this

work, I also collected data for leaf area index as well as sap flow rate of 5 different slash pine trees.

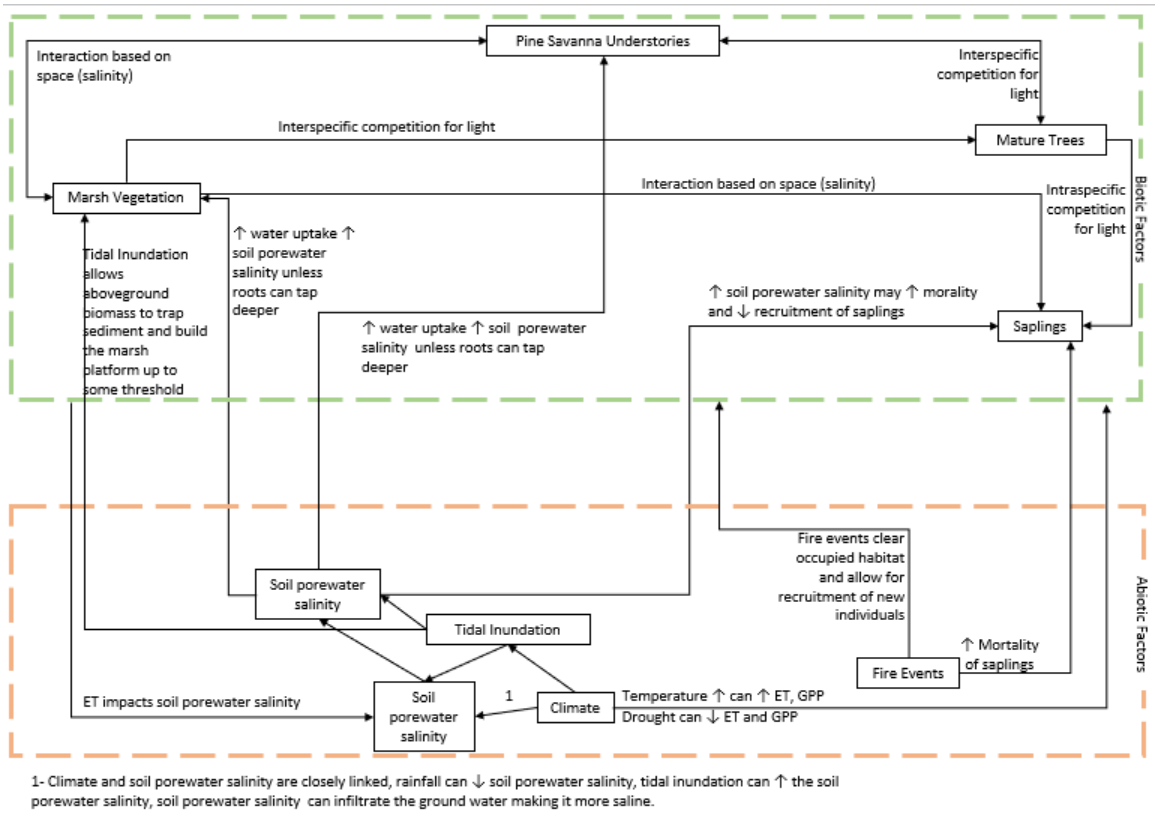

Figure 3.1 *Conceptual model showing the four functional groups (saplings, mature trees, marsh vegetation, and pine savanna vegetation) and their relation to abiotic factors*

REFERENCES

Adam, P. (1990). *Saltmarsh ecology*. Cambridge University Press.

Alldred, M., Liberti, A., & Baines, S. B. (2017). Impact of salinity and nutrients on salt marsh stability. *Ecosphere*, *8*(11), e02010.

Anderson, J. R. (1976). *A land use and land cover classification system for use with remote sensor data* (Vol. 964). US Government Printing Office

Battaglia, L. L., Woodrey, M. S., Peterson, M. S., Dillon, K. S., & Visser, J. M. (2012). Wetlands of the northern gulf coast. *Wetland Habitats of North America: Ecology and Conservation Concerns*, *January*, 75–88. https://doi.org/10.1525/9780520951419-008

Barbier, E. B., Georgiou, I. Y., Enchelmeyer, B., & Reed, D. J. (2013). The value of wetlands in protecting southeast Louisiana from hurricane storm surges. *PloS one*, *8*(3), e58715

Barbier, E. B., Hacker, S. D., Kennedy, C., Koch, E. W., Stier, A. C., & Silliman, B. R. (2011). The value of estuarine and coastal ecosystem services. *Ecological monographs*, *81*(2), 169-193.

Borchert, S. M., Osland, M. J., Enwright, N. M., & Griffith, K. T. (2018). Coastal wetland adaptation to sea level rise: Quantifying potential for landward migration and coastal squeeze. *Journal of applied ecology*, *55*(6), 2876-2887.

Bourne, J. (2000). Louisiana's vanishing wetlands: Going, going... *Science*, *289*(5486), 1860-1863.

Brinson, M. M., Christian, R. R., & Blum, L. K. (1995). Multiple states in the sea-level induced transition from terrestrial forest to estuary. *Estuaries*, *18*(4), 648-659.

Burns, C. J., Alber, M., & Alexander, C. R. (2021). Historical changes in the vegetated area of salt marshes. *Estuaries and Coasts*, *44*(1), 162-177.

Christmas, J.Y. (1973).Cooperative Gulf of Mexico Estuarine Inventory and Study Mississippi. Gulf Coast Research Laboratory, Ocean Springs, Mississippi (434 pp).

Clark, J. S. (2005). Why environmental scientists are becoming Bayesians. *Ecology letters*, *8*(1), 2-14.

Conner, W., Whitmire, S., Duberstein, J., Stalter, R., & Baden, J. (2022). Changes within a South Carolina Coastal Wetland Forest in the Face of Rising Sea Level. *Forests*, *13*(3), 414.

Costanza, R., d'Arge, R., De Groot, R., Farber, S., Grasso, M., Hannon, B., Limburg, K., Naeem, S., O'Neill, R.V., Paruelo, J., Raskin, R.G., Sutton, P., van den Belt, M., (1997). The value of the world's ecosystem services and natural capital. *nature*, *387*(6630), 253-260

Cowardin, L. M. (1979). *Classification of wetlands and deepwater habitats of the United States*. Fish and Wildlife Service, US Department of the Interior.

Dahl, T. E., & Stedman, S. M. (2013). Status and trends of wetlands in the coastal watersheds of the Conterminous United States 2004 to 2009.

Dai, A. & National Center for Atmospheric Research Staff (Eds). Last modified 12 Dec 2019. "The Climate Data Guide: Palmer Drought Severity Index (PDSI)." Retrieved from https://climatedataguide.ucar.edu/climate-data/palmer-drought-severity-index-pds

Donnelly, J. P., & Bertness, M. D. (2001). Rapid shoreward encroachment of salt marsh cordgrass in response to accelerated sea-level rise. *Proceedings of the National Academy of Sciences*, *98*(25), 14218-14223.

Eastman, J. R. (1987). *TerrSet Manual*. www.clarklabs.org

Eleuterius, C. K., & Criss, G. A. (1991). Point aux Chenes: Past, Present, and Future Perspective of Erosion. *Ocean Springs, Mississippi: Physical Oceanography Section Gulf Coast Research Laboratory*.

Eleuterius, L. N., & Eleuterius, C. K. (1979). Tide levels and salt marsh zonation. *Bulletin of Marine science*, *29*(3), 394-400.

Elsey-Quirk, T., Graham, S. A., Mendelssohn, I. A., Snedden, G., Day, J. W., Twilley, R. R., Shaffer, G., Sharp, L. A., Pahl, J., & Lane, R. R (2019). Mississippi river sediment diversions and coastal wetland sustainability: Synthesis of responses to freshwater, sediment, and nutrient inputs. *Estuarine, Coastal and Shelf Science*, *221*, 170-183.

Engle, V. D. (2011). Estimating the provision of ecosystem services by Gulf of Mexico coastal wetlands. *Wetlands*, *31*(1), 179-193.

Environmental Protection Agency. (2015). *Coastal Wetlands Initiative: Gulf of Mexico Review*.

Field, D. W. (1991). *Coastal wetlands of the United States: An accounting of a valuable national resource* (Vol. 55). National Oceanic and Atmospheric Administration.

Field, C. R., Gjerdrum, C., & Elphick, C. S. (2016). Forest resistance to sea-level rise prevents landward migration of tidal marsh. *Biological Conservation*, *201*, 363-369.

Glenn, E. P., Mexicano, L., Garcia-Hernandez, J., Nagler, P. L., Gomez-Sapiens, M. M., Tang, D., Lomeli, M. A., Ramirez-Hernandez, J., & Zamora-Arroyo, F. (2013). Evapotranspiration and water balance of an anthropogenic coastal desert wetland: Responses to fire, inflows and salinities. *Ecological engineering*, *59*, 176-184.

Grand Bay National Estuarine Research Reserve. (2013). www.grandbaynerr.org228-475-7047

Haglöf Inc. Haglöf Electric Clinometer. https://www.forestry-suppliers.com/Documents/1760_msds.pdf

Hardy, T. (2018). Coastal Wetland Dynamics Under Sea-level Rise and Wetland Restoration in the Northern Gulf of Mexico using Bayesian Multilevel Models and a Web Tool.

Hardy, T., Wu, W., & Peterson, M. S. (2021). Analyzing spatial variability of drivers of coastal wetland loss in the northern Gulf of Mexico using Bayesian multi-level models. *GIScience & Remote Sensing*, *58*(6), 831-851.

Hilbert, K. W. (2006). Land cover change within the grand bay national estuarine research reserve: 1974–2001. *Journal of Coastal Research*, *22*(6), 1552-1557.

Hooten, M. B., & Hobbs, N. T. (2015). A guide to Bayesian model selection for ecologists. Ecological monographs, 85(1), 3-28.

Hsieh, Y. P. (2004). Dynamics of tidal salt barren formation and the record of present-day sea level change. *The Ecogeomorphology of Tidal Marshes. Coastal and Estuarine Studies*, *59*.

Jackson, D. (2012). Headliners: Mississippi's Pascagoula River Designated as a Model River in America's Great Outdoor Rivers Program.

Jankowski, K. L., Törnqvist, T. E., & Fernandes, A. M. (2017). Vulnerability of Louisiana's coastal wetlands to present-day rates of relative sea-level rise. *Nature Communications*, *8*(1), 1-7.

Kearney, W. S., Fernandes, A., & Fagherazzi, S. (2019). Sea-level rise and storm surges structure coastal forests into persistence and regeneration niches. *PloS one*, *14*(5), e0215977.

Kirwan, M. L., & Gedan, K. B. (2019). Sea-level driven land conversion and the formation of ghost forests. *Nature Climate Change*, *9*(6), 450-457.

Kirwan, M. L., Guntenspergen, G. R., d'Alpaos, A., Morris, J. T., Mudd, S. M., & Temmerman, S. (2010). Limits on the adaptability of coastal marshes to rising sea level. *Geophysical research letters*, *37*(23).

Kirwan, M. L., Kirwan, J. L., & Copenheaver, C. A. (2007). Dynamics of an estuarine forest and its response to rising sea level. *Journal of Coastal Research*, *23*(2), 457-463.

Kirwan, M. L., & Megonigal, J. P. (2013). Tidal wetland stability in the face of human impacts and sea-level rise. *Nature*, *504*(7478), 53-60.

Kirwan, M. L., Temmerman, S., Skeehan, E. E., Guntenspergen, G. R., & Fagherazzi, S. (2016). Overestimation of marsh vulnerability to sea level rise. *Nature Climate Change*, *6*(3), 253-260.

Larjavaara, M., & Muller-Landau, H. C. (2013). Measuring tree height: a quantitative comparison of two common field methods in a moist tropical forest. *Methods in Ecology and Evolution*, *4*(9), 793-801.

Lellis-Dibble, K. A., McGlynn, K. E., & Bigford, T. E. (2008). Estuarine fish and shellfish species in US commercial and recreational fisheries: economic value as an incentive to protect and restore estuarine habitat.

Lindsey, R. (2020). *Climate Change: Global Sea Level*. Climate.gov. Retrieved April 4, 2022, from https://www.climate.gov/news-features/understanding-climate/climate-change-global-sea-level.

Linscombe, R. G., & Hartley, S. B. (2011). *Analysis of change in marsh types of coastal Louisiana, 1978-2001*.

Lowery G.H. Jr., Newman R.J. (1954). The birds of the Gulf of Mexico. In Gulf of Mexico: its origin, waters, and marine life, Galtsoff PS, editor. Washington, DC: USFWS, pp. 519–4

Mogensen, L. A., & Rogers, K. (2018). Validation and comparison of a model of the effect of sea-level rise on coastal wetlands. *Scientific reports*, *8*(1), 1-14.

Monk, C. D. (1968). Successional and environmental relationships of the forest vegetation of north central Florida. *American Midland Naturalist*, 441-457.

Morris, J. T. (1995). The mass balance of salt and water in intertidal sediments: results from North Inlet, South Carolina. *Estuaries*, *18*(4), 556-567.

Morris, J. T., Edwards, J., Crooks, S., & Reyes, E. (2012). Assessment of carbon sequestration potential in coastal wetlands. In *Recarbonization of the biosphere* (pp. 517-531). Springer, Dordrecht.

Nicholson, H. M. (2017). Textural Analysis of Historical Aerial Photography to Determine Change In Coastal Marsh Extent: Site of the Present-Day Grand Bay National Estuarine Research Reserve (GBNERR), Mississippi, 1955-2014.

NOAA National Centers for Environmental information, Climate at a Glance: Statewide Time Series, published June 2022, retrieved on June 17, 2022 from https://www.ncdc.noaa.gov/cag/

NOAA Tides and Currents. (n.d.). Relative Sea Level Trend 8747437 Bay Waveland, Mississippi. Retrieved May 1, 2022, from https://tidesandcurrents.noaa.gov/sltrends/sltrends_station.shtml?id=8747437

Orson, R., Panageotou, W., & Leatherman, S. P. (1985). Response of tidal salt marshes of the US Atlantic and Gulf coasts to rising sea levels. *Journal of Coastal Research*, 29-37.

Partyka, M. L., & Peterson, M. S. (2008). Habitat quality and salt-marsh species assemblages along an anthropogenic estuarine landscape. *Journal of Coastal Research*, *24*(6), 1570-1581.

Penland, S., & Ramsey, K. E. (1990). Relative sea-level rise in Louisiana and the Gulf of Mexico: 1908-1988. *Journal of Coastal Research*, 323-342.

Peterson, M. S., Waggy, G. L., & Woodrey, M. S. (2007). *Grand Bay national estuarine research reserve: An ecological characterization*. Grand Bay National Estuarine Research Reserve.

Raabe, E. A., & Stumpf, R. P. (2016). Expansion of tidal marsh in response to sea-level rise: Gulf Coast of Florida, USA. *Estuaries and Coasts*, *39*(1), 145-157.

Risser, P. G. (1995). The status of the science examining ecotones. *BioScience*, *45*(5), 318-325.

Sacatelli, R., Lathrop, R., & Kaplan, M. B. (2020). Impacts of climate change on coastal forests in the northeast US.

Schieder, N. W., Walters, D. C., & Kirwan, M. L. (2018). Massive upland to wetland conversion compensated for historical marsh loss in Chesapeake Bay, USA. *Estuaries and coasts*, *41*(4), 940-951.

Sharma, A., Brethauer, D. K., McKeithen, J., Bohn, K. K., & Vogel, J. G. (2020). Prescribed burn effects on natural regeneration in pine flatwoods: Implications for uneven-aged stand conversion from a Florida study. *Forests*, *11*(3), 328.

Shepard, C. C., Crain, C. M., & Beck, M. W. (2011). The protective role of coastal marshes: a systematic review and meta-analysis. *PloS one*, *6*(11), e27374.

Shirley, L. J., & Battaglia, L. L. (2006). Assessing vegetation change in coastal landscapes of the northern Gulf of Mexico. *Wetlands*, *26*(4), 1057-1070.

Stedman, S. M., & Dahl, T. E. (2008). Status and trends of wetlands in the coastal watersheds of the eastern United States, 1998 to 2004.

Stephenson, N. L., Das, A. J., Condit, R., Russo, S. E., Baker, P. J., Beckman, N. G., Coomes, D. A., Lines, E. R., Morris, W. K., Rüger, N., Álvarez, E., Blundo, C., Bunyavejchewin, S., Chuyong, G., Davies, S. J., Duque, Á., Ewango, C. N., Flores, O., Franklin, J. F., Grau, H.R., Hao, Z., Harmon, M. E., Hubbell, S. P., Kenfack, D., Lin, Y., Makana, J. R., Malizia, A., Malizia, L. R., Pabst, R. J., Pongpattananurak, N., Su, S. H., Sun, I. F., Tan, S., Thomas, D., van Mantgem, P. J., Wang, X., Wiser, S. K., & Zavala, M. A. (2014). Rate of tree carbon accumulation increases continuously with tree size. *Nature*, *507*(7490), 90-93.

Sweet, W. V., Hamlington, B. D., Kopp, R. E., Weaver, C. P., Barnard, P. L., Bekaert, D., Brooks, W., Craghan, M., Dusek, G., Frederikse, T., Garner, G., Genz, A. S., Krasting, J. P., Larour, E., Marcy, D., Marra, J. J., Obeysekera, J., Osler, M.,

Pendleton, M., Roman, D., Schmied, L., Veatch, W., White, K. D., & Zuzak, C. (2022). *Global and regional sea level rise scenarios for the United States: Updated mean projections and extreme water level probabilities along US coastlines* (No. 01). NOAA Technical Report.

Terrano, J. (2018). *An evaluation of marsh shoreline erosion and sediment deposition in the Grand Bay National Estuarine Research Reserve, Mississippi, USA*. University of South Florida.

U.S. Geological Survey. (2016). National Water Information System data available on the World Wide Web (USGS Water Data for the Nation), accessed April 4, 2022, at URL https://maps.waterdata.usgs.gov/mapper/index.html

Waldron, M. C. B., Carter, G. A., & Biber, P. D. (2021). Using aerial imagery to determine the effects of sea-level rise on fluvial marshes at the mouth of the Pascagoula River (Mississippi, USA). *Journal of Coastal Research*, *37*(2), 389-407.

Wang, H., Hsieh, Y. P., Harwell, M. A., & Huang, W. (2007). Modeling soil salinity distribution along topographic gradients in tidal salt marshes in Atlantic and Gulf coastal regions. *Ecological modelling*, *201*(3-4), 429-439.

Wang, J., Church, J. A., Zhang, X., & Chen, X. (2021). Reconciling global mean and regional sea level change in projections and observations. *Nature communications*, *12*(1), 1-12.

Wasson, K., Woolfolk, A., & Fresquez, C. (2013). Ecotones as indicators of changing environmental conditions: rapid migration of salt marsh–upland boundaries. *Estuaries and Coasts*, *36*(3), 654-664.

Wieland, Ronald, Mike Duran, Barry McPhail, and Bruce Sorrie. 1998. Rare species, habitat types and associated ecological communities of the proposed Grand Bay National Estuarine Research Reserve. Museum Technical Report No. 61, Vol. 1 - Report and Maps. 53 pp; Vol. 2 - Appendices - Conservation ranking, plant lists, and field notes. Mississippi Museum of Natural Science, Mississippi Natural Heritage Program, Jackson, Mississippi.

Więski, K., Guo, H., Craft, C. B., & Pennings, S. C. (2010). Ecosystem functions of tidal fresh, brackish, and salt marshes on the Georgia coast. *Estuaries and Coasts*, *33*(1), 161-169.

Wu, W., Biber, P., Mishra, D. R., & Ghosh, S. (2020). Sea-level rise thresholds for stability of salt marshes in a riverine versus a marine dominated estuary. *Science of the Total Environment*, *718*, 137181.

Wu, W., Biber, P. D., Peterson, M. S., & Gong, C. (2012). Modeling photosynthesis of Spartina alterniflora (smooth cordgrass) impacted by the Deepwater Horizon oil spill using Bayesian inference. *Environmental Research Letters*, *7*(4), 045302.

Youngflesh, C. (2018). MCMCvis: Tools to visualize, manipulate, and summarize MCMC output, J Open Source Softw 3:640. https://doi.org/10.21105/joss.00640.